

Titre: Comparison of the Renishaw Ball Bar and Samba Method in 3-Axis and 5-Axis Machine Calibration, Including Reversal Error Estimation with the Tango Method
Title:

Auteur: Irfaan Mohammed
Author:

Date: 2019

Type: Mémoire ou thèse / Dissertation or Thesis

Référence: Mohammed, I. (2019). Comparison of the Renishaw Ball Bar and Samba Method in 3-Axis and 5-Axis Machine Calibration, Including Reversal Error Estimation with the Tango Method [Mémoire de maîtrise, Polytechnique Montréal]. PolyPublie.
Citation: <https://publications.polymtl.ca/4105/>

 **Document en libre accès dans PolyPublie**
Open Access document in PolyPublie

URL de PolyPublie: <https://publications.polymtl.ca/4105/>
PolyPublie URL:

Directeurs de recherche: J. R. René Mayer
Advisors:

Programme: Génie mécanique
Program:

POLYTECHNIQUE MONTRÉAL

affiliée à l'Université de Montréal

Comparison of the Renishaw Ball Bar and Samba Method in 3-Axis and 5-Axis Machine Calibration, Including Reversal Error Estimation with the Tango Method

X MOHAMMED IRFAAN

Département de génie mécanique

Mémoire présenté en vue de l'obtention du diplôme de *Maîtrise ès sciences appliquées*

Génie mécanique

Décembre 2019

POLYTECHNIQUE MONTRÉAL

affiliée à l'Université de Montréal

Ce mémoire intitulé :

Comparison of the Renishaw Ball Bar and Samba Method in 3-Axis and 5-Axis Machine Calibration, Including Reversal Error Estimation with the Tango Method

présenté par x **MOHAMMED IRFAAN**

en vue de l'obtention du diplôme de Maîtrise ès sciences appliquées

a été dûment accepté par le jury d'examen constitué de :

Marek BALAZINSKI, président

René MAYER, membre et directeur de recherche

Farbod KHAMENEIFAR, membre

DEDICATION

To my family

ACKNOWLEDGMENTS

I want to express my gratitude to my research supervisor professor Rene Mayer for giving me this opportunity to do research and support, guidance, and suggestion during my research work. Without his excellent guidance and supervision, it was never possible to finalize this research. His office door was always open for me whenever I had urgent enquires.

I am thankful to Mr. Vincent Mayer and Mr. Guy Gironne to perform the experimental work; without their support, it was challenging to finish this work.

At last, I am heartily thankful to my family for their patience and support during my studies.

RÉSUMÉ

Cette étude porte sur la comparaison des erreurs géométriques de la fraiseuse 5 axes obtenues par l'analyse d'une barre à billes Renishaw avec celles de la méthode SAMBA/TANGO.

Les vingt paramètres de l'erreur recueillis par le logiciel de la barre à billes Renishaw dans les plans XY, YZ, et ZX sont le jeu d'inversion, le jeu latéral, la rectitude, l'erreur d'échelle, et la perpendicularité selon X, Y et Z.

Une stratégie composée développée pour la méthode TANGO/SAMBA utilise 21 indexations, une échelle et quatre sphères calibrées, et une face. La face est mesurée plusieurs fois avec différents pré-mouvements selon X, Y et Z pour identifier l'erreur de retournement et l'erreur de jeu d'inversion.

Les résultats montrent que les paramètres de l'erreur sont comparables en utilisant les deux méthodes. Le paramètre associé à l'erreur d'échelle EXX montre des valeurs d'erreur cohérentes. L'erreur d'échelle vaut $-4.65\ \mu\text{m}$ et $-4.67\ \mu\text{m}$ pour la méthode barre à billes et la méthode SAMBA/TANGO respectivement.

Cette nouvelle technique qui a été développée pour estimer l'erreur de retournement et aussi utilisée dans ce projet pour déterminer l'erreur de six retournement. L'erreur de quatre retournement était en accord avec la méthode de Renishaw barre à billes et celle de SAMBA/TANGO.

Globalement, les données acquises montrent que la comparaison des méthodes BB et SAMBA/TANGO est possible pour 9 des 20 paramètres d'erreur.

ABSTRACT

This research work is related to the comparison of the geometric error of the HU40T five-axis machine tool obtained with a Renishaw ball bar with those from the SAMBA/ TANGO method.

The twenty-error parameter gathered from the Renishaw ball bar software in the XY, YZ, and ZX plane are backlash error, lateral play, straightness, scaling error, and squareness error in the X, Y, and Z direction.

A compound strategy developed for the SAMBA/ TANGO method uses 21-indexations, one scale and four master balls, and one facet. The reversal and backlash error measured by repeatedly probing the facet with different pre-motion in X, Y, and Z-axis

Finally, the result of the present work shows that the error parameter are not always in good agreement between these two methods. The scaling error parameter in the x-direction EXX was in close agreement. Scaling error values found at $-4.65\ \mu\text{m}$ and $-4.67\ \mu\text{m}$ in Ball bar and SAMBA/TANGO, respectively.

The new technique developed for the estimation of reversal error was useful to obtain the six-reversal error. The four-reversal error was in agreement for the Renishaw ball bar and SAMBA/ TANGO method.

The overall obtained measured data shows that the comparison of the Renishaw ball bar and SAMBA/TANGO method is possible for the 9-error parameter out of the 20-selected parameter.

TABLE OF CONTENTS

DEDICATION	III
ACKNOWLEDGMENTS.....	IV
RÉSUMÉ.....	V
ABSTRACT	VI
TABLE OF CONTENTS	VII
LIST OF TABLES	XI
LIST OF FIGURES.....	XII
LIST OF ABBREVIATIONS	XV
LIST OF APPENDICES	XVI
CHAPTER 1 INTRODUCTION.....	1
1.1 Problem Introduction.....	1
1.2 Research questions	1
1.3 Objectives.....	1
1.4 Research approach.....	2
1.5 Outline of the thesis.....	2
CHAPTER 2 LITERATURE REVIEW	3
2.1 Introduction	3
2.2 Error description of machine tool.....	3
2.2.1 Motion Error (Intra Axis).....	3
2.2.2 Link Error (Inter axis error or axis location and orientation).....	5
2.2.3 The thermal error of the machine tool.....	6
2.2.4 Volumetric Error	7
2.3 Review of existing methods and approaches	7

2.4	Direct method	7
2.5	Indirect method	8
2.5.1	RUMBA, SAMBA, and TANGO	12
2.6	Summary of Literature Review	17
CHAPTER 3 EXPERIMENTAL WORK AND METHODOLOGY		18
3.1	The SAMBA and TANGO Test.....	18
3.2	Applied strategy	20
3.2.1	SAMBA simulator.....	22
3.3	Ball bar test.....	23
3.3.1	YZ and ZX Plane Test.....	23
3.3.2	XY plane Test.....	25
3.4	Straightness Error measurement.....	26
3.5	Backlash error measurement	27
3.6	Scaling error measurement.....	27
3.7	Squareness error measurement.....	28
CHAPTER 4 REVERSAL ERROR MEASUREMENT		30
4.1	Reversal error measurement including Pre movement	30
4.1.1	Reversal Error EXYb and EXZb.....	30
4.1.2	Reversal Error EZXb and EYZb	32
4.1.3	Reversal Error EYXb and EYZb.....	33
CHAPTER 5 RESULT ANALYSIS		36
5.1	Error analysis.....	36
5.1.1	Backlash error in the X direction (EXXb)	36
5.1.2	Backlash error in the Y direction (EYYb)	37

5.1.3	Reversal Error (EXYb).....	39
5.1.4	Reversal Error (EYXb).....	40
5.1.5	Reversal Error (EYZb)	42
5.1.6	Reversal Error (EZYb).....	43
5.1.7	Reversal Error (EZXB)	45
5.1.8	Reversal Error (EXZb)	46
5.1.9	Straightness error of X-axis in Y direction (EYX)	48
5.1.10	Straightness error of X-axis in the Z direction (EZX)	49
5.1.11	Straightness error of Y-axis in the X direction (EXY).....	51
5.1.12	Straightness error of Y-axis in the Z direction (EZY)	52
5.1.13	Straightness error of Z-axis in the X direction (EXZ)	54
5.1.14	Straightness error of Z-axis in the Y direction (EYZ)	55
5.1.15	Linear positioning error motion of X-axis (EXX)	57
5.1.16	Linear positioning error motion of Y-axis (EYY)	59
5.1.17	Linear positioning error motion of Z-axis (EZZ).....	61
5.1.18	Squareness Error EXZ1	62
5.1.19	Squareness Error ECZ0 and ECX0	64
5.2	Correlation.....	65
5.2.1	Backlash correlation	65
5.2.2	Lateral play correlation	66
5.2.3	Straightness correlation	68
5.2.4	Scaling error correlation.....	69
5.2.5	Squareness error correlation.....	70
CHAPTER 6	DISCUSSION	72

CHAPTER 7	CONCLUSION AND RECOMMENDATION	75
REFERENCES		77
APPENDICES		80

LIST OF TABLES

Table 2.1: Error notation of X-axis	4
Table 2.2: Potential error notation of A, B, C-axis	5
Table 2.3: Before and after calibration results	11
Table 3.1: SAMBA/TANGO Strategy	20
Table 3.2: Workpiece SAMBA Balls and TANGO Face Position	21
Table 3.3: Error parameter notation in SAMBA/TANGO and ball bar method	29
Table 4.1: Reversal error Pre-movement direction	32
Table 4.2: Mean error and standard measured values by BB and by S/T method	35
Table 7.1: Renishaw Ball bar analyzed the result	80
Table 7.2: SAMBA/ TANGO analyzed the result	81

LIST OF FIGURES

Figure 2.1: Motion error of linear axis and rotary axis (ISO230-1, 2012).....	4
Figure 2.2: Link error of C axis (Jiang & Cripps, 2015).....	5
Figure 2.3: Link error of A-axis (Jiang & Cripps, 2015)	6
Figure 2.4: Effect of temperature on a machine tool (Mayr et al., 2012)	6
Figure 2.5: Positioning error measurement by a laser interferometer (Schwenke et al., 2008)	7
Figure 2.6: Straightness interferometer with Wollaston prism and bi-mirror (Schwenke et al., 2008)	8
Figure 2.7: Cap Ball setup (Zargarbashi & Mayer, 2009)	9
Figure 2.8: Experimental setup with a probed point at A and C axes (Ibaraki et al., 2012b)	10
Figure 2.9: Chase the ball method (Bringmann & Knapp, 2006)	11
Figure 2.10: Three dimensional ball plate (Liebrich et al., 2009).....	12
Figure 2.11: Rumba Setup (Mayer, 2012).....	13
Figure 2.12: Experimental Setup for TANGO (Mayer et al., 2015)	13
Figure 2.13: Fixed Magnetic ball bar (Bryan, 1982).....	15
Figure 2.14: Graphical representation of machine error (Renishaw, 2001-2019)	16
Figure 2.15: Machine error and their causes (Renishaw, 2001-2019)	17
Figure 3.1: SAMBA and TANGO error measurement setup.....	18
Figure 3.2: A view of TANGO method	19
Figure 3.3: Indexation angle.....	21
Figure 3.4: Process to estimate error parameter in the SAMBA simulator.....	22
Figure 3.5: Process to measure the error parameter in post-processor.....	23
Figure 3.6: Ball Bar YZ-plane test	24

Figure 3.7: Ball Bar ZX-plane test	24
Figure 3.8: Ball Bar XY-plane test.....	25
Figure 3.9: Straightness error EYX.....	26
Figure 4.1: Probing movement reversal error EXYb and EXZ.....	31
Figure 4.2: Probing movement reversal error EZXb and EZYb	33
Figure 4.3: Reversal error EYXb and EYZb.....	34
Figure 5.1: Error Parameter EXXb	37
Figure 5.2: Error Parameter EYYb	38
Figure 5.3: Error Parameter EXYb	40
Figure 5.4: Error Parameter EYXb	41
Figure 5.5: Error Parameter EYZb.....	43
Figure 5.6: Error Parameter EZYb.....	44
Figure 5.7: Error Parameter EZXb.....	46
Figure 5.8: Error Parameter EXZb.....	47
Figure 5.9: Representation of error parameter EYX.....	49
Figure 5.10: Representation of error parameter EZX	50
Figure 5.11: Representation of error parameter EXY	52
Figure 5.12: Representation of error parameter EZY	53
Figure 5.13: Representation of error parameter EXZ	55
Figure 5.14: Representation of error parameter EYZ	56
Figure 5.15: Representation of error parameter EXX.....	58
Figure 5.16: Representation of error parameter EYY	60
Figure 5.17: Representation of error parameter EZZ.....	62
Figure 5.18: Representation of error parameter EXZ1	63

Figure 5.19: Representation of error parameter ECZ0 and ECX0	64
Figure 5.20: Backlash correlation between BB and S/T method	66
Figure 5.21: Lateral play error correlation between S/T and BB method	67
Figure 5.22: Straightness error correlation between S/T and BB method	69
Figure 5.23: Scaling error correlation between S/T and BB method	70
Figure 5.24: Squareness error correlation between S/T and BB method	71

LIST OF ABBREVIATIONS

SAMBA	Scale and Master Ball Artefact
TANGO	Touch and Go
S/T	SAMBA and TANGO
BB	Ball Bar

LIST OF APPENDICES

APPENDICE A EXPERIMENTAL DATA SUMMARY	80
---	----

CHAPTER 1 INTRODUCTION

The five-axis machine tool is in high demand in the aerospace industries because of their high production rate. The machines with additional B (A) and C axis cut the multiple parts; these multiple-axis machines increase the production rate. Part accuracy is a significant factor in the aerospace industries during the machining process. Finished parts are affected by possible errors such as geometric error, dynamic error, kinematic error, error due to force on the tool, and thermal error.

1.1 Problem Introduction

The machine tools have errors such as geometric error, dynamic error, loading error, and thermal error. The present work provides a correlation study for the geometric error of the five-axis machine tool using two different measurement methods, such as the SAMBA/ TANGO and Ball bar method.

1.2 Research questions

There is no work on the comparison of geometric error measurement of the five-axis machine tool for different calibration approaches as well as estimation of the reversal error for the five-axis machine. As a result, the main aim of this research work is to compare the SAMBA/ TANGO method and Renishaw ball bar. The research questions are as follows:

How to estimate the geometric error parameters using the SAMBA/TANGO method and commercially available Renishaw ball bar software?

Which error parameters correspond in the S/T method and Renishaw ball bar?

How to measure the reversal error using the TANGO method?

Are the two methods providing similar error parameter values?

1.3 Objectives

The main objective of this study is to correlate the geometric error of the five-axis machine using the scale and master ball (SAMBA), touch and go method (TANGO), and Renishaw ball bar test. Moreover, the specific objectives of this research are as follows:

- i. To measure the geometric error of the five-axis HU40T machine tool using the SAMBA/TANGO method and Renishaw ball bar software.
- ii. To estimate the reversal error using the TANGO approach.
- iii. Determine the correlation between the SAMBA/TANGO, and ball bar approaches.

1.4 Research approach

In the present work, the first phase is to develop the SAMBA and TANGO strategy to measure the geometric error with an appropriate G code. Prepare the machine pallet as an artifact for the SAMBA and TANGO approaches and perform the experimental work. Then conduct the Renishaw ball bar experiment for the XY, YZ, and, ZX plane. Finally, compare the estimated parameter.

1.5 Outline of the thesis

In the present work, a total seven-chapter are included named introduction, literature review, experimental work & methodology, reversal error estimation, result analysis, discussion, and last chapter was the conclusion.

The introduction chapter provides detail about the flow of this research work, including research questions, objectives, and research approaches. The second chapter highlights the experimental work and developed methods and reflects the measurement procedure of machine error with different apparatus and procedures. The SAMBA/TANGO and Renishaw ball bar experiment and strategy used for SAMBA/TANGO method were explained in chapter 3. The developed new technique for reversal error measurement explained in Chapter 4. The obtained experimental data observed and presented graphically and statically in Chapter 5. Finally, a discussion and conclusion presented in chapter 6 and chapter 7.

CHAPTER 2 LITERATURE REVIEW

2.1 Introduction

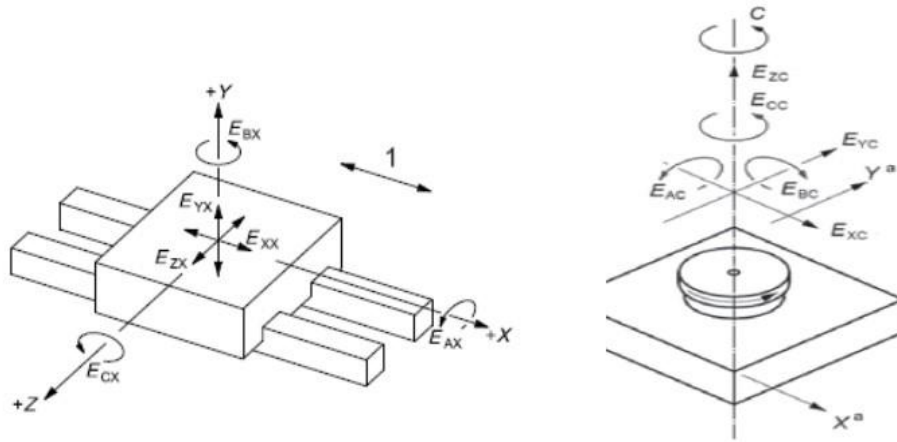
Multi-axis machine tools provide the high accuracy machined part in less time and at high speed because of the fast movement of the linear and rotary axis. This section analyzes the literature of the machine tool error and error calibration process, as well as the precision of five-axis machines, and the influence of an error on the machine tools were discussed. Different error measuring methods, such as direct and indirect methods, are presented. For the direct calibration approaches, previously, researchers used laser interferometer, straightness interferometer, and angular interferometer.

On the other hand, The R-test device, 'model chase the ball,' scale and master ball method (SAMBA), touch and go (TANGO), 3D probe ball, and ball plate artifact were used for indirect methods. The first section of this chapter explains the different types of error of a five-axis machine tool. Then error compensation procedures, including direct and indirect methods, will be discussed.

2.2 Error description of machine tool

2.2.1 Motion Error (Intra Axis)

The intra axis error is also known as Position dependent geometric error (PDGE). If the structural part of the machine such as guideway and column are inaccurate, PDGEs affect the machine tool accuracy. Intra axis includes three translation and three angular error, for instance, yaw, pitch, and roll, as shown in Figure 2.1. (Abbaszadeh-Mir, Mayer, Cloutier, & Fortin, 2002; Jiang & Cripps, 2015)



Where

1 X-Axis commanded linear motion

E_{AX} angular error motion around A-axis (roll)

E_{BX} angular error motion around B-axis (yaw)

E_{CX} angular error motion around C-axis (pitch)

E_{XX} linear positioning error motion of X axis

E_{YX} straightness error motion in Y-axis direction

E_{ZX} straightness error motion in Z-axis direction

E_{XC} radial error motion of C in X- direction

E_{YC} radial error motion of C in Y- direction

E_{ZC} axial error motion of C

E_{AC} tilt error motion of C around X-axis

E_{BC} tilt error motion of C around Y-axis

E_{CC} angular positioning error motion of C

Figure 2.1: Motion error of linear axis and rotary axis (ISO230-1, 2012)

Table 2.1: Error notation of X-axis

Linear Position error	Straightness error	Angular error
E_{XX}	E_{YX}	E_{AX}
—	E_{ZX}	E_{BX}
—	—	E_{CX}
E_{YY}	E_{XY}	E_{AY}
—	E_{ZY}	E_{BY}
—	—	E_{CY}
E_{ZZ}	E_{XZ}	E_{AZ}
—	E_{YZ}	E_{BZ}
—	—	E_{CZ}

Where E = error

XX = First letter denotes the direction of error

XX = Second letter shows the mechanical axis having such an error

2.2.2 Link Error (Inter axis error or axis location and orientation)

Link error is also extensively noted by Position independent geometric error (PIGE). Link error occurs owing to the inaccurate assembly process of the five-axis machine tool. These errors affect the location of the axis. (Jiang & Cripps, 2015). To anticipate the position and orientation error of the five-axis machine tool, mainly, it has 12 axis location errors. On each axis, it has eight PIGEs (Abbaszadeh-Mir et al., 2002).

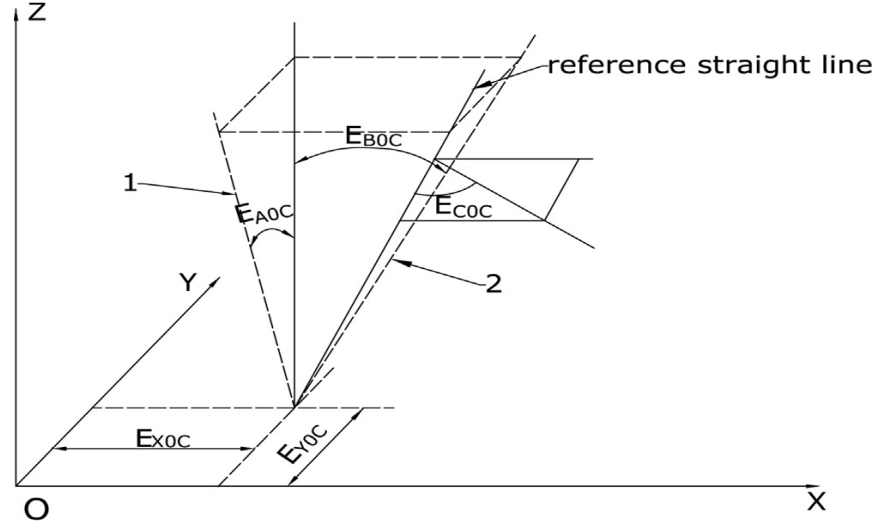


Figure 2.2: Link error of C axis (Jiang & Cripps, 2015)

Table 2.2: Potential error notation of A, B, C-axis

Linear position error	Orientation error	Zero position
E_{YOA}	E_{BOA}	E_{AOA}
E_{ZOA}	E_{COA}	--
E_{XOB}	E_{AOB}	E_{BOB}
E_{ZOB}	E_{COB}	--
E_{XOC}	E_{AOC}	E_{COC}
E_{YOC}	E_{BOC}	--

Table 2.2 shows the inter axis error of A, B, C axis.

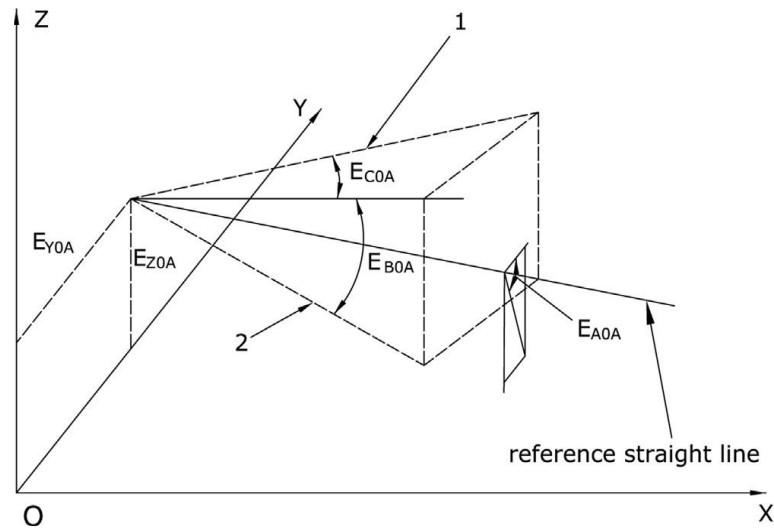


Figure 2.3: Link error of A-axis (Jiang & Cripps, 2015)

2.2.3 The thermal error of the machine tool

Machine tools and their factors are affected by the change in temperatures such as coefficient of thermal expansion gradient and dissimilitude of temperature and spatial & temporal boundaries of temperature. A machine tool bed affected by temperature, shown in Figure 2.4. This bending generates several errors in the machine tool and affects the machine part accuracy. (Mayr et al., 2012)

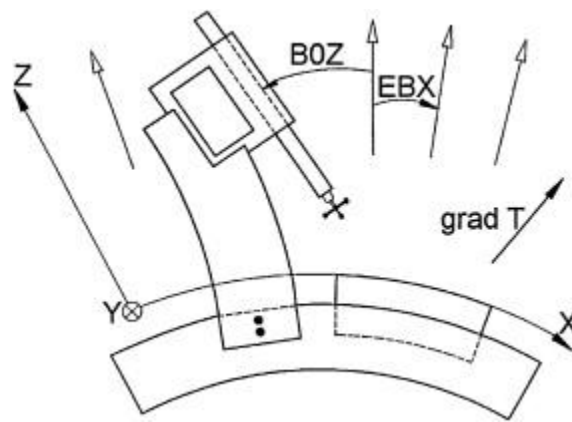


Figure 2.4: Effect of temperature on a machine tool (Mayr et al., 2012)

2.2.4 Volumetric Error

The diagonal displacement test measures the volumetric performance of the machine tool (ISO230-1, 2012). The position-dependent geometric error, position-independent geometric error, as well as quasi-static error, and a thermal error occurred due to the Volumetric errors (Xing, Mayer, & Achiche, 2018).

2.3 Review of existing methods and approaches

Many researchers have studied direct and indirect error measuring methods; highly skilled personnel is required to arrange the setup of additional devices on a selected machine tool for the direct method. On the other hand, for indirect approaches, researchers prefer to use the probe with a different design of artifacts and strategies.

2.4 Direct method

The direct method of measurement usually uses a laser interferometer, as shown in Figure 2.5 and different devices such as line scale, calibrated scale, gauge block, step gauge, and encoder system to measure the positioning errors. These errors are related to both geometry and the driven axis of the machine. (ISO230-1, 2012; Schwenke et al., 2008)

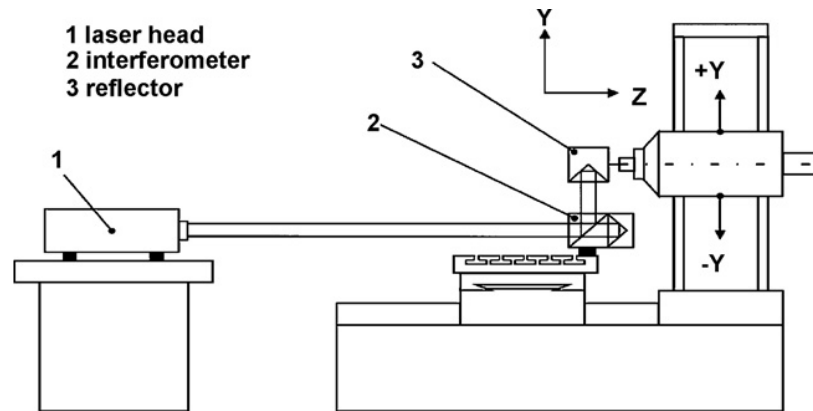


Figure 2.5: Positioning error measurement by a laser interferometer (Schwenke et al., 2008)

On the other hand, a laser interferometer also uses to measure straightness error. It has Wollaston prism and a bi-mirror reflector. As shown in Figure 2.6, when the laser passes through straightness optic, it divides the laser into two different parts, and again both joined at straightness reflector to

measure the displacement by producing an interference signal. (ISO230-1, 2012; Schwenke et al., 2008)

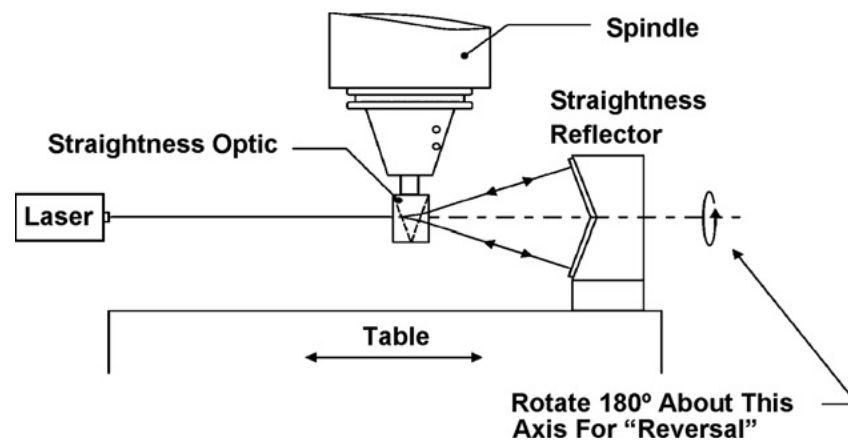


Figure 2.6: Straightness interferometer with Wollaston prism and bi-mirror (Schwenke et al., 2008)

2.5 Indirect method

Different techniques were introduced for the indirect method, some of utilizing direct method devices such as auto-alignment laser interferometer, Laser ball bar (LLB), Grid bar device (Chen, Kou, & Chiou, 1999; Srinivasa & Ziegert, 1996). A telescopic magnetic ball bar used to measure the eight-position independent geometric error parameter (PIGEP) of the five-axis machine tool. The kinematic model of homogenous transformation matrices was developed for the machine tool. Jacobian matrices played an important role in minimizing the error parameter up to 8 link errors (Abbaszadeh-Mir et al., 2002). In another major study, the author proposed a single setup method with a double ball bar to identify axis motion error of the five-axis machine with the 'A' axis. The author did five sensitive tests and observe that in ball bar data, it has radius variation due to setup error (Zargarbashi & Mayer, 2006). Later on (Zargarbashi & Mayer, 2009), utilize a 3D cap ball device to measure the eight link error. It consists of a master ball and a sensing head. As shown in Figure 2.7, the sensing head attached to the spindle with a tool holder while the master ball placed on the machine table. This combined setup is called 'Cap Ball.' Jacobian matrices model have used for the mathematical analysis, and the author concluded that leading machine error was a B-C axis distance of 120 μm and the B axis tilt around x of 49 $\mu\text{m}/\text{m}$.

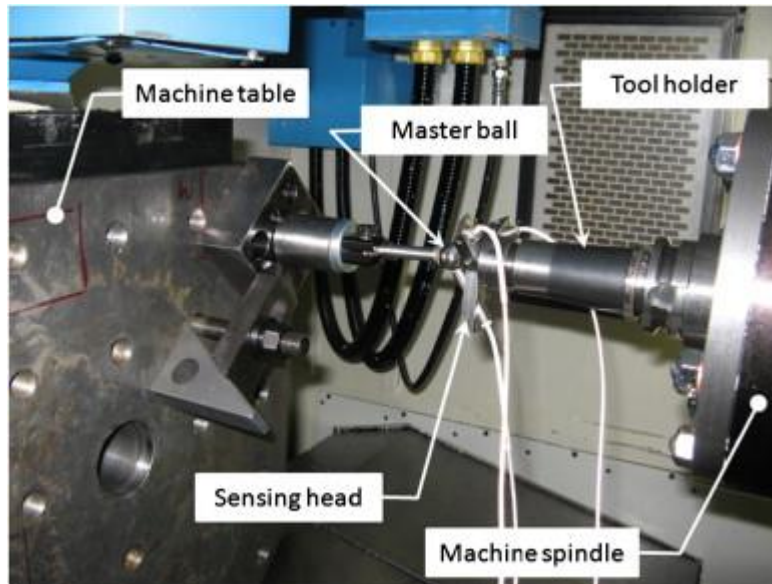


Figure 2.7: Cap Ball setup (Zargarbashi & Mayer, 2009)

Another interesting work where the author adopted cone frustum from NAS (National Aerospace Standard) 979, it is famous around the manufacturer to get the performance of a machine tool. The R-test was used to measure the motion and link error of the B and C axis. After the measurement, it finally concluded that the B axis has its influence on the C axis in terms of motion error and verified that in cone frustum test C axis has a high impact for circularity error. (Hong, Ibaraki, & Matsubara, 2011). In an investigation into the five-axis machine tool, the Author installed a touch probe RMP-60 by the Renishaw plc, on machine spindle to calibrate rotary axis location error. Author mounted trial piece, as shown in Figure 2.8 on the machine table, and marked 28 touch points on this trial piece. (Ibaraki, Iritani, & Matsushita, 2012a, 2012b)

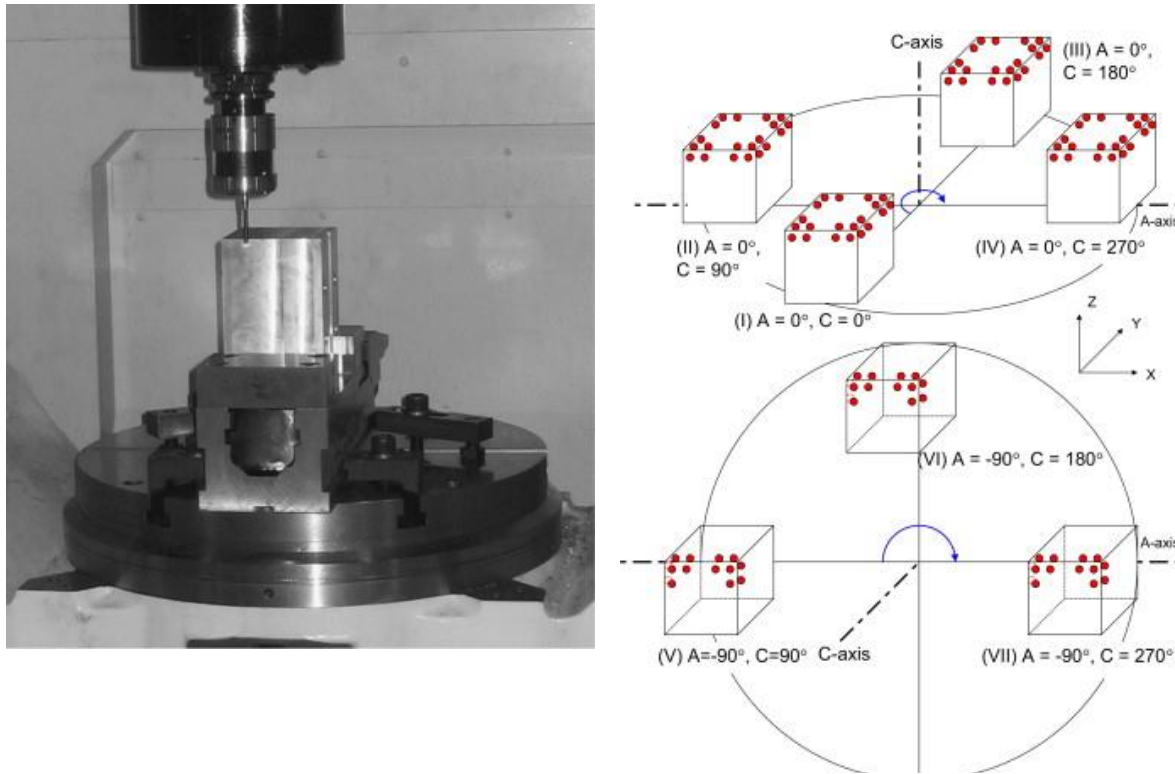


Figure 2.8: Experimental setup with a probed point at A and C axes (Ibaraki et al., 2012b)

The R-test device introduced by (Weikert, 2004) for the measurement of the five-axis machine tool. It is an assembly of three analog probes placed on the machine table with a tilt angle. The measurement was taken by rotating the C axis in both clockwise and counterclockwise directions at 260 mm in diameter. The author used 42 error parameters, and the time taken by this method for the error measurement was 20 minutes. On the other hand, the best result was a straightness error reduced by 210 to 33 μm .

(Bringmann & Knapp, 2006) Developed a model-based “chase the ball” that utilizes one holder placed on the machine table, on this holder four linear probes were attached. The tool center point shown by a ceramic precision sphere probe was attached to the spindle of the machine, 79 measuring indexations were used by movement of linear axis and rotary axis to complete the test total, A-axis were limited from -95 degree to +25 degree, and the C axis had distributed over 360 degrees for measuring indexation.

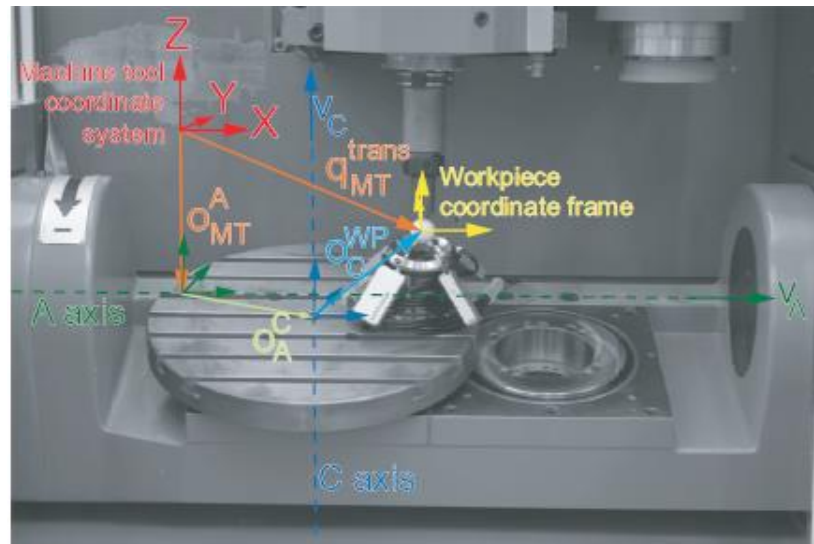


Figure 2.9: Chase the ball method (Bringmann & Knapp, 2006)

The author concluded that with different calibration strategies, the performance of the machine tool could be measured by the Monte Carlo method. This method also suggests that calibration quality could not verify, so the researcher used a 3D circular test with double ball bar to verify the quality before and after calibration as shown in below Table 2.3

Table 2.3: Before and after calibration results

Test	Unidirectional mean diameter deviation	Circular form deviation
Before calibration	+106 μm / +100 μm	-14 μm / -19 μm
After calibration	39 μm / 45 μm	25 μm / 33 μm

Detailed work of (Bringmann, Küng, & Knapp, 2005) built a three-dimensional artifact with a working volume of 500 mm x 500 mm x 150 mm for CMM calibration; it has 6x6 aluminum oxide spheres to be made up of nominal diameter 22 mm and nominal pitch 200 mm as indicates in Figure 2.10. Three prisms were installed on the base plate, as suggested by (Hale & Slocum, 2001). (Liebrich, Bringmann, & Knapp, 2009) used a reversal method that means coordinate of ball plate separated from machine error and concluded that this new artifact was able to measure the three-axis machine error, and no rotational axis used, determine the measurement uncertainty less than 5 μ m. (Liebrich et al., 2009), utilize the same artifact via the working volume of 500 mm x 500 mm x 320 mm to determine the squareness error, straightness error for X, Y, and Z-axis. As per the result, measured the uncertainty 2.1 μ m for the X and Y-axis and 1.5 μ m in the Z direction.

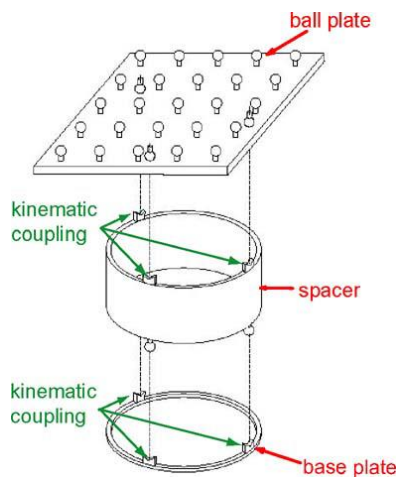


Figure 2.10: Three dimensional ball plate (Liebrich et al., 2009)

2.5.1 RUMBA, SAMBA, and TANGO

A new artifact was employed by (Erkan, Mayer, & Dupont, 2011) with different height of rods, master balls attached on each rod to make the three-dimensional structure. These rods directly screwed to the machine table. The method called reconfigurable uncalibrated master balls artifact (RUMBA) proposed to measure the volumetric distortion in the five-axis machine tool topology of wCBXFZYt. The Reconfigurable uncalibrated master ball artifact (RUMBA) were enriched by (Mayer, 2012), where carbon fiber tubes and fixed ball bars of 304.6686 mm in length used to design atifact. The author used 24 ceramic balls, have a diameter of 12.7 mm each, which are placed on fiber tubes, as shown in Figure 2.11. In the beginning, the SAMBA method was able to determine the 13 error parameters, which consist of 10 location errors and three linear axis errors.

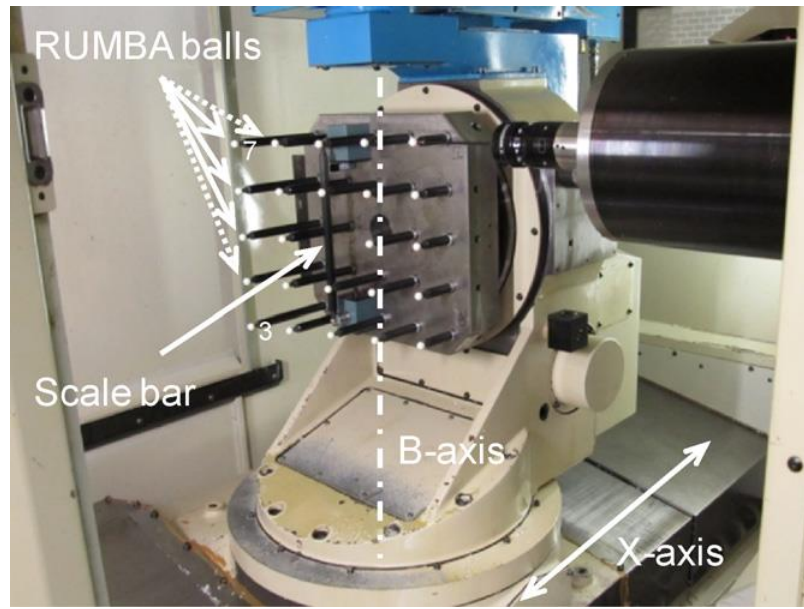


Figure 2.11: Rumba Setup (Mayer, 2012)

Afterward (Mchichi & Mayer, 2014) enriched the SAMBA method by introducing the measurement of error motion factor, where 84 axis location error and error motion coefficient recognized. This enrichment is also helpful in decreasing the quantity of master ball on the artifact, and it decreased the machine calibration time. Previously (Mayer, 2012), the SAMBA method used only to measure axis location error. (Mayer, Rahman, & Los, 2015) used the 'A' axis to be made an artifact on the five-axis machine tool. The artifact is 500 mm in diameter, as shown in Figure 2.12 a for the estimation of eight positions independent geometric error by bringing into touch the probe on curved and flat facets.

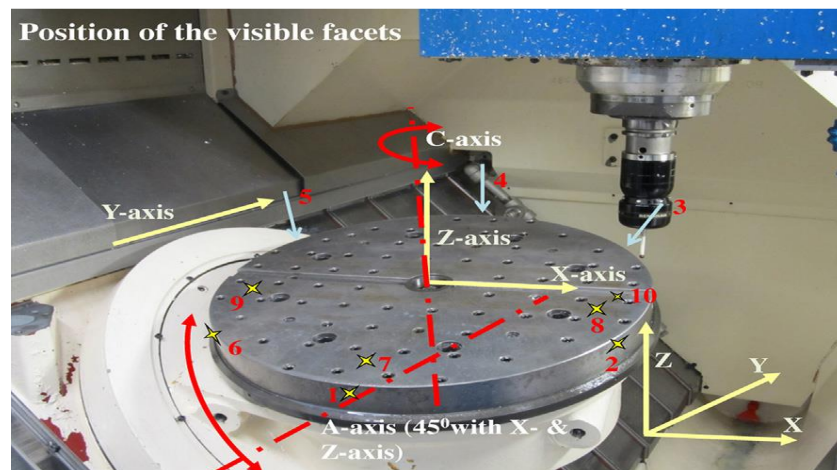


Figure 2.12: Experimental Setup for TANGO (Mayer et al., 2015)

A new concept was developed by (Rahman & Mayer, 2015), where a machine table itself used to create an uncalibrated artifact. In this artifact, 26 facets were specially created on the machine table for the measurement of PDGE and PIGE. A face brought in contact with a touch probe than another facet fetched for the continuous process; this process is known as TANGO or 'TOUCH AND GO' method. The privilege of this technique is that it does not need any external artifact. Recently (Xing, Achiche, Esmaili, & Mayer, 2018) used a laser interferometer and SAMBA method to estimate the linear positioning error of the five-axis machine tool, the interferometer was mounted on the spindle and C axis was equipped with the reflector to complete the experiment. The author concludes that both the error range and value were close to each other. For instance, the value for the X-axis was 1.5 μm , and Y-axis was 4.9 μm (Xing, Achiche, et al., 2018). Meanwhile, (Xing, Achiche, & Mayer, 2019) published an article in which the original work was related to C-axis machine pallet change. The author measured 13 error parameters and found that there were no significant changes in volumetric error due to machine pallet change. However, during the maximum movement of a linear axis, it has some variation in scaling error around 3 to 4 μm (Xing et al., 2019)

Many research was done for the calibration of the five-axis machine tool using a double ball bar so far. The ball bar by Renishaw is a conventional device to calibrate the machine tool, and there are two spheres mounted on both sides of the bar. For the measuring purpose, the ball bar rotated in both clockwise and counterclockwise directions than evaluate the difference between computed lengths, known as a machine error. As illustrated in Figure 2.13, it has a fixed and free socket. To calibrate the machine, free socket and fixed socket mounted on machine spindle and table, respectively. (Bryan, 1982).

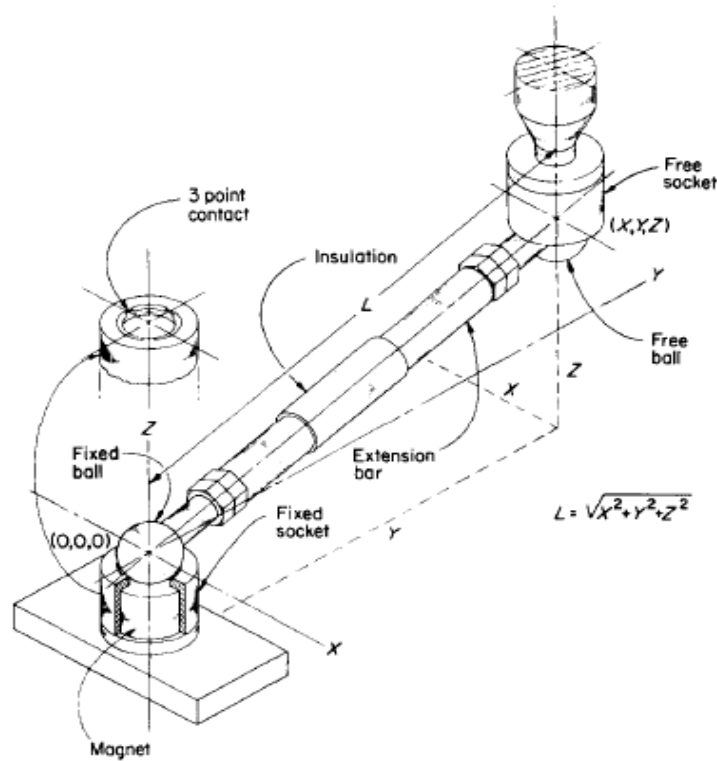


Figure 2.13: Fixed Magnetic ball bar (Bryan, 1982)

The Renishaw ball bar can present the result of the computed machine in graphical form with Ball bar 20 software. Machine error behavior of XY, YZ, and ZX plane could present in various international standard formats such as ASME B5.54/ B5.57, ISO 230-4, JIS B 6190, GB/T 17421.4 and the Renishaw layout itself. It does not require any external CNC Program to run the test. The program can develop according to their specific machine controller. The software arranges the error in the ranking system as per their effect on the machine so the user can easily understand which parameter has a maximum and minimum impact on the machine tool (Renishaw, 2001-2019).

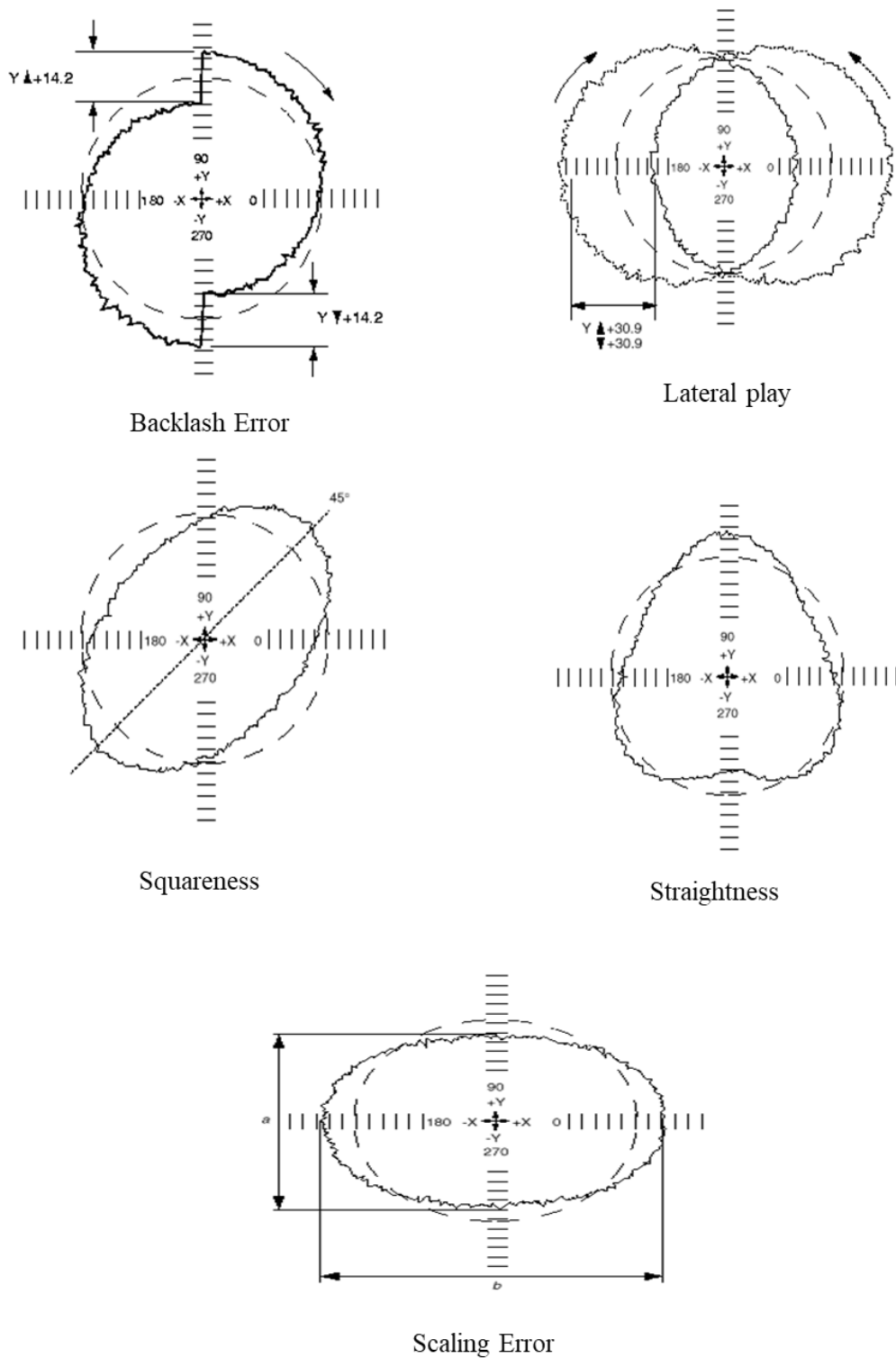


Figure 2.14: Graphical representation of machine error (Renishaw, 2001-2019)

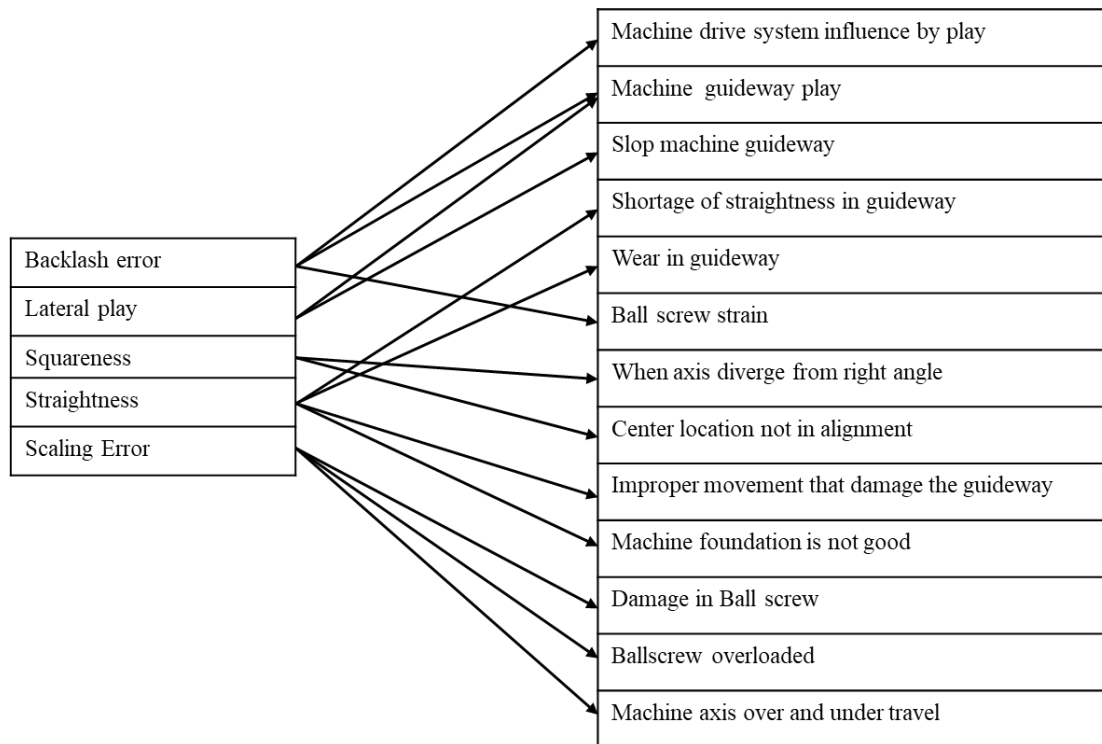


Figure 2.15: Machine error and their causes (Renishaw, 2001-2019)

2.6 Summary of Literature Review

This research review focused on the trend of five-axis machine calibration and looked at the different approaches developed. To estimate the geometric error, thermal error, and dynamic error, many works were accomplished on the direct and indirect calibration methods.

However, the question arises that is it possible to compare the error parameter of the Renishaw ball bar with SAMBA and TANGO methods?

The present work can address this question. For this reason, the author selected the error parameter comparison between the SAMBA/TANGO method and the commercially available Renishaw software.

CHAPTER 3 EXPERIMENTAL WORK AND METHODOLOGY

This section described the experimental work for the SAMBA / TANGO and ball bar. The tests were performed on a horizontal five-axis CNC machine of Mitsui Seiki HU40T, and the machine structure is wCBXfYZt.

The experiments were performed on this machine tool for the SAMBA/TANGO, and ball bar (XY, YZ, and ZX plane) tests. Before the actual test machine had two hours and 15 minutes warm-up running in order to bring the machine in stable condition.

First, the SAMBA/ TANGO tests were performed then initialize the setup for the XY, YZ, and ZX plane to perform the ball bar test and compare all possible geometric errors using the SAMBA/TANGO and ball bar methods.

3.1 The SAMBA and TANGO Test

In the present research work, both SAMBA and TANGO techniques are implemented on the machine to measure the geometric error parameter. For each SAMBA/TANGO test, it took one hour 40 minutes with the strategy, as shown in Table 3.1.

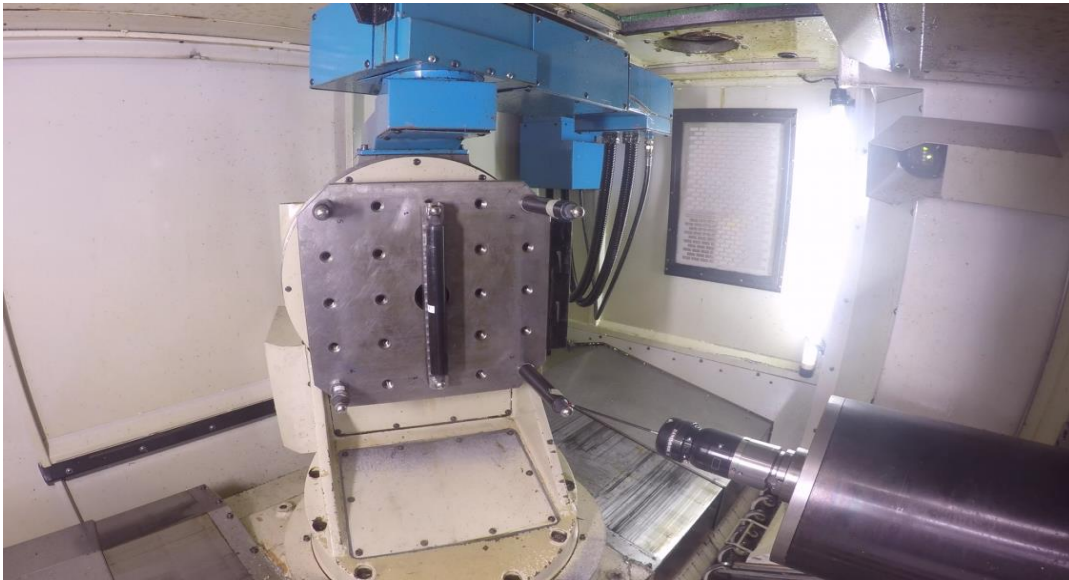


Figure 3.1: SAMBA and TANGO error measurement setup

The SAMBA artifact utilizes different height rods with a ball radius of 9.55 mm mounted on the machine pallet is shown in Figure 3.1. A Renishaw probe mounted on the HU40T machine spindle is used to measure the center of the ball.

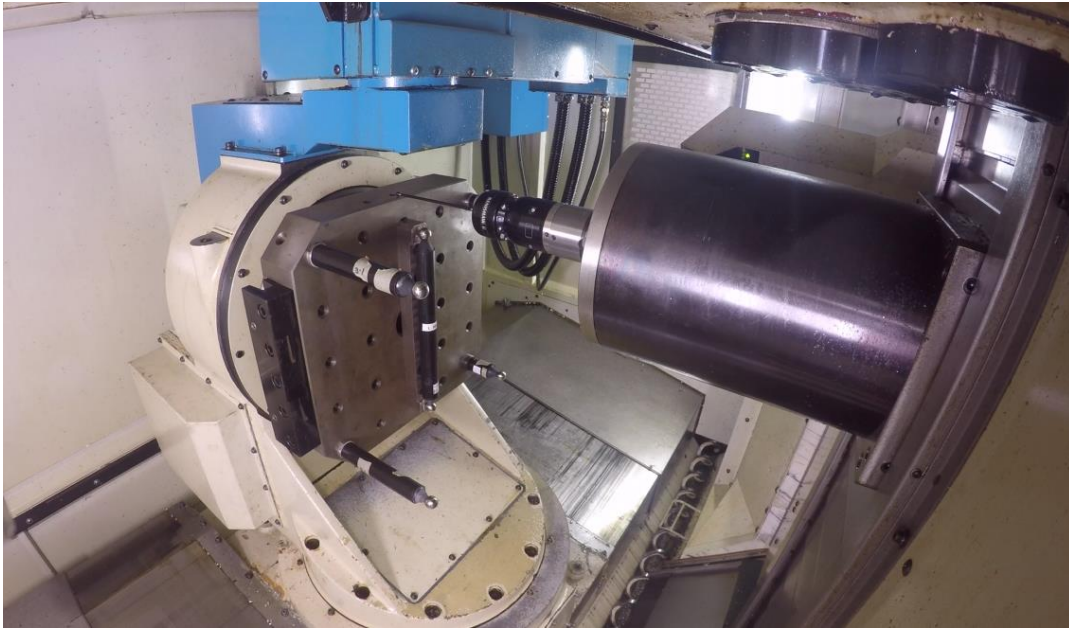


Figure 3.2: A view of TANGO method

For the TANGO method, continuously facets were probed. In this work, a single touch facet used for probing to get the reversal error in the X, Y, and Z directions as well as backlash error in X and Y direction. During the touch and go method, indexation has pre-movement in x, y, and z-direction. Pre-movement helps to obtain reversal and backlash errors. The Renishaw probe is used to touch the facet for different rotary axis indexation angles as per Table 3.1.

Table 3.1: SAMBA/TANGO Strategy

Indexation number	A, B and C Axis rotation angle			Measurable SAMBA Balls and TANGO facet
1	0	10	30	'3 4 5'
2	0	-10	-30	'3 4 5'
3	0	30	90	'3 4 5'
4	0	-30	-90	'3 4 5'
5	0	50	150	'3 4 5'
6	0	-50	-150	'3 4 5'
7	0	70	210	'3 4 5'
8	0	-70	-210	'3 4 5'
9	0	90	270	'3 4 5 6'
10	0	-90	-270	'3 4 5 6'
11	0	60	180	'3 4 5'
12	0	-60	-180	'3 4 5'
13	0	40	120	'3 4 5'
14	0	-40	-120	'3 4 5'
15	0	20	60	'3 4 5'
16	0	-20	-60	'3 4 5'
17	0	0	0	'1 2 3 4 5 6 7 7 7 7''
18	0	-90	0	'7 7 7 7'
19	0	0	90	'7 7 7 7'
20	0	0	180	'7 7 7 7'
21	0	0	-90	'7 7 7 7'

3.2 Applied strategy

Table 3.2 shows the position of the six balls and one facet that brings in for the probing purposes. As shown in Table 3.1, a total of 21 indexations were considered. Additionally, 76 points have probed for both the SAMBA and TANGO technique. According to indexation, C and B axis were rotating in the clockwise and counterclockwise direction in order to determine all possible error parameters.

To measure the backlash and lateral play error in X, Y, and Z direction facet has measured repetitively four times with 10 mm pre-movement in all three directions.

Table 3.2: Workpiece SAMBA Balls and TANGO Face Position

Balls and face Identity	Position		
	X	Y	Z
Ball 1	-152.4	0	40.855
Ball 2	+152.4	0	40.435
Ball 3	160.0	160.0	177.835
Ball 4	-160.0	160.0	177.695
Ball 5	-160.0	-160.0	75.605
Ball 6	160.0	-160.0	76.045
Facet 1	200.0	0	-10.0

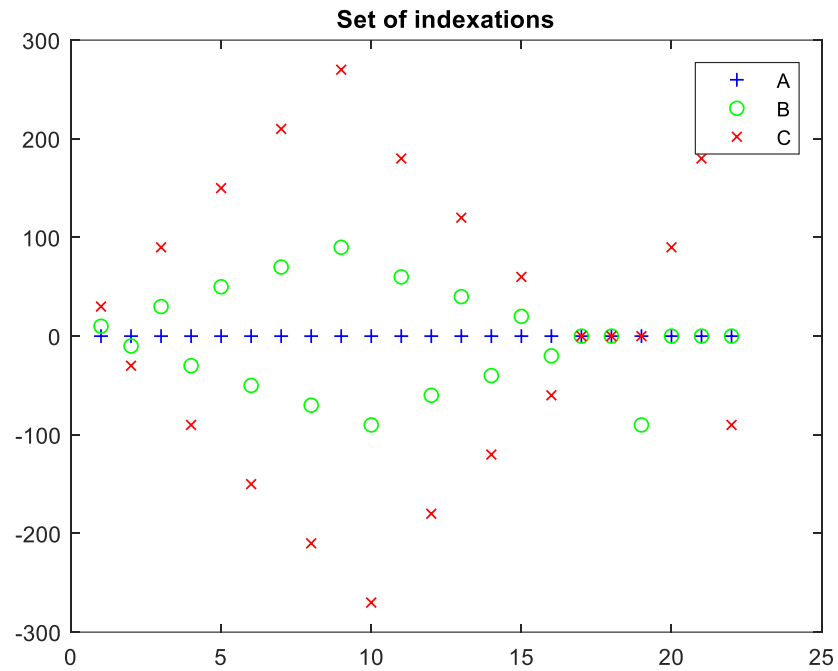


Figure 3.3: Indexation angle

The graph shows the actions of B and C indexation on the machine tool; this strategy has taken place in all four tests. The angle used in the strategy was in positive and negative sequence, as clear from Table 3.1.

3.2.1 SAMBA simulator

In this work, The AxiSAMBA software was used to simulate the geometric error of the HU40T machine tool. The SAMBA simulator has two-step to analyses the machine probing data. In the first step, the user has to define the ball and facet location and follow the process according to Figure 3.4. The generated G-code from step one is used to run the machine with some modification as follows by step 2, illustrated in Figure 3.5.

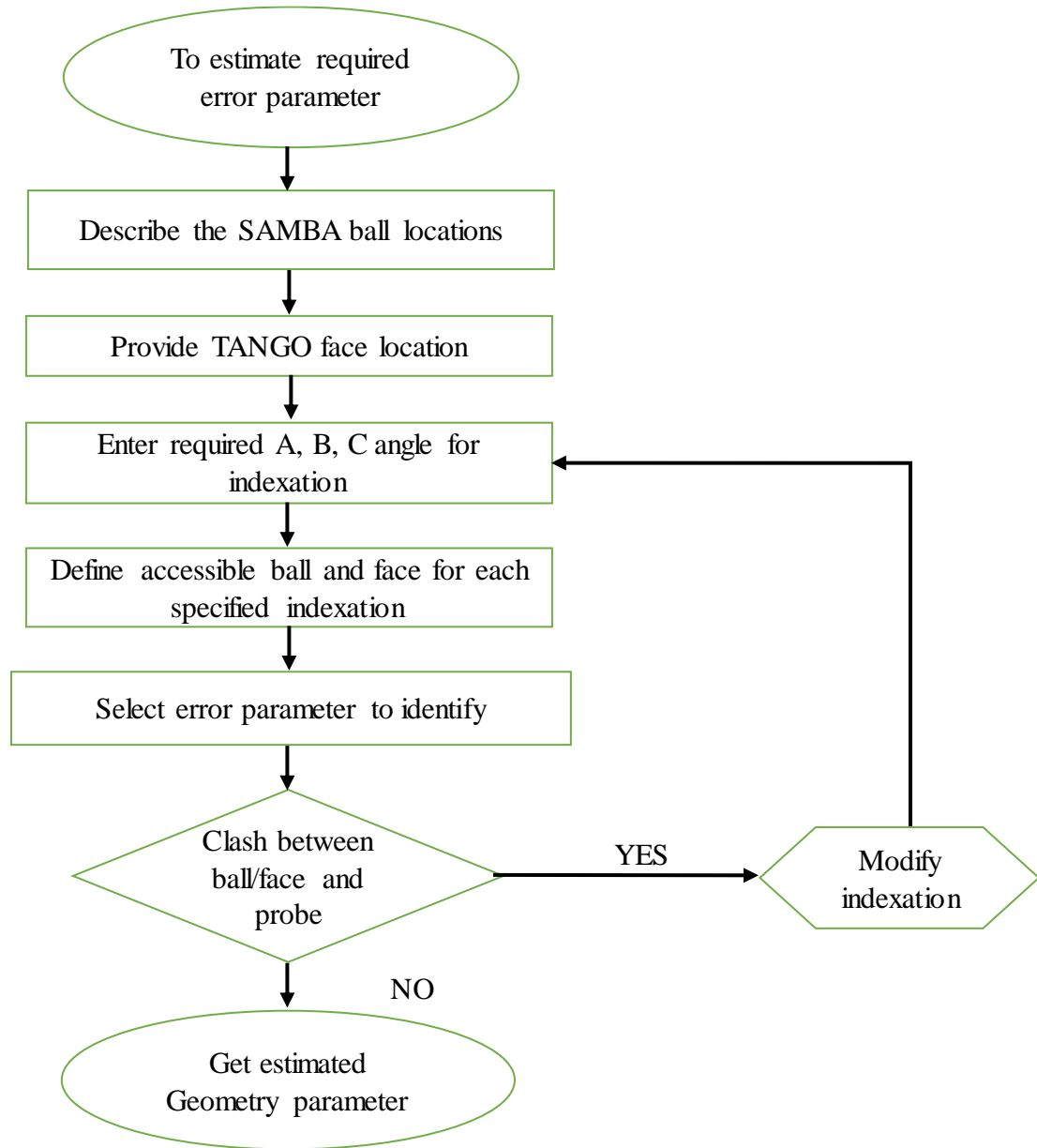


Figure 3.4: Process to estimate error parameter in the SAMBA simulator

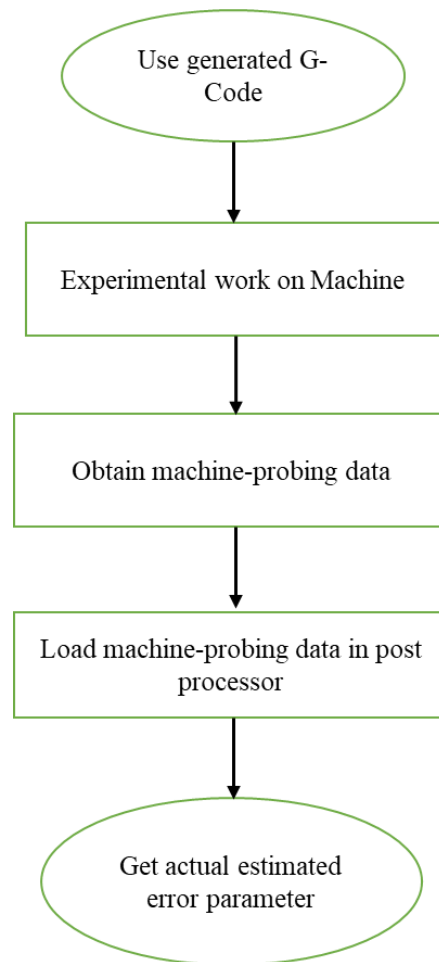
Step 2

Figure 3.5: Process to measure the error parameter in post-processor

3.3 Ball bar test

The Ball bar classic test was carried out on the HU40T horizontal five-axis Machine tool. The Renishaw ball bar used and the test radius was 150 mm.

3.3.1 YZ and ZX Plane Test

As illustrated in Figure 3.6, ball bar tests were done to measure the error parameter and get the analytical result from the Renishaw ball bar software. Earlier, as shown in Figure 3.2, the pallet

has the master ball and scale ball installed on it. On the other hand, the ball bar test pallet has changed, and a fixture is installed on the pallet for ZX and YZ test, as shown in Figure 3.6 and Figure 3.7.

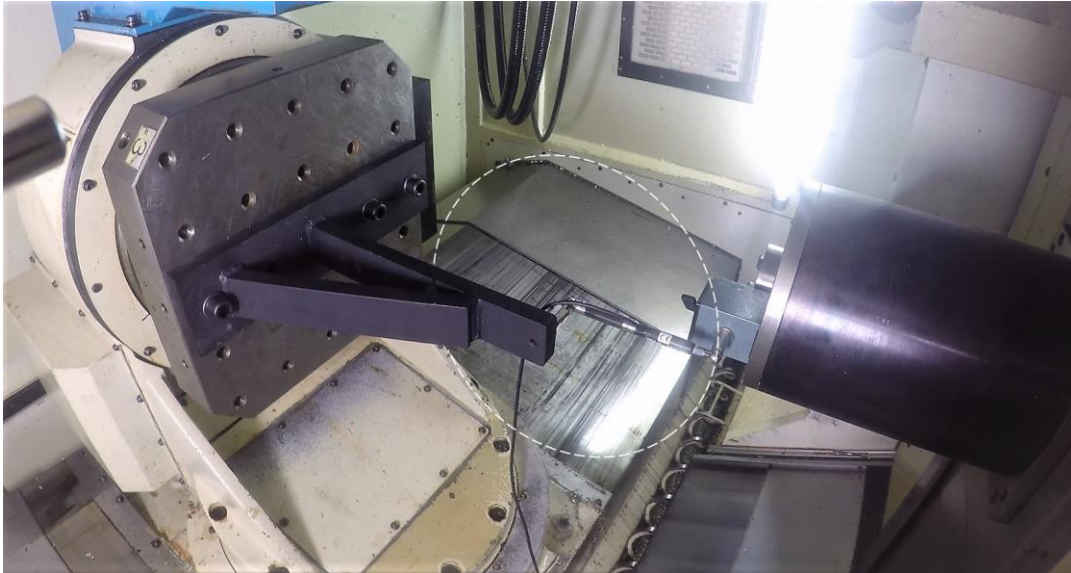


Figure 3.6: Ball Bar YZ-plane test

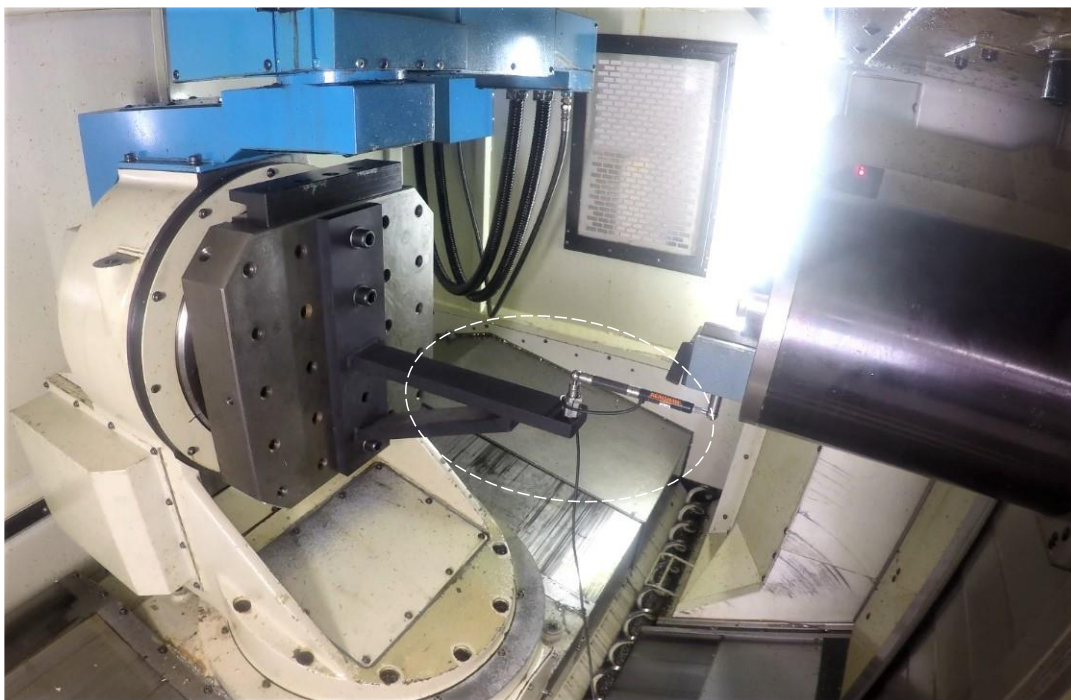


Figure 3.7: Ball Bar ZX-plane test

As it is clear from Figure 3.6. The additional setup used in this experiment for ZX and YZ tests. The fixture of length 315 mm is placed on the machine workpiece table, and the ball bar workpiece ball is mounted on the fixture with a magnetic block. The ball bar tool ball is attached to the spindle with a magnetic block.

For the ZX test, the ZX plane has selected from the Renishaw software, and the machine table angle was $A=0^\circ$, $B=0^\circ$, and $C=0^\circ$. The machine movement was limited to only the Z and the X machine axis. The machine pallet can move in X direction negative and positive for the estimation of the error parameter in the XZ plane.

A similar fixture was used for the YZ test, but the machine pallet position was changed from $A=0^\circ$, $B=0^\circ$, and $C=0^\circ$ to $A=0^\circ$, $B=0^\circ$, and $C=90^\circ$. For the YZ plane test, the used G code restricts the movement of the machine X-axis. In this setup, the machine pallet was not able to move in any direction. To complete the test in a clockwise direction and counterclockwise direction as required for the ball bar test, machine spindle has the Z-axis and Y-axis movement in a negative and positive direction.

3.3.2 XY plane Test

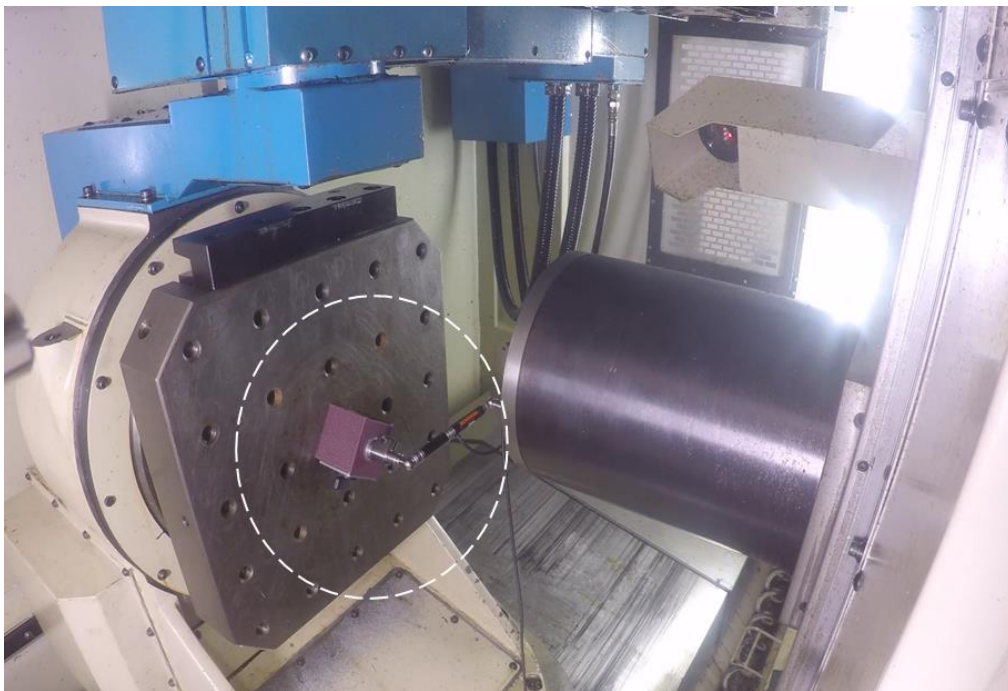


Figure 3.8: Ball Bar XY-plane test

For instance, as shown in Figure 3.8, the XY plane test performed to measure the error parameter. Workpiece ball attached to a block placed on the center of the C axis pallet and tool ball is attached to the horizontal machine spindle.

Now it is an XY plane test, the machine pallet was able to move in negative and positive X direction as well as machine spindle in the Y direction. The test performs in back to back clockwise and counterclockwise direction to get the error values.

3.4 Straightness Error measurement

From Equation 3.1, the second-order term $E_{YX2} * x^2$ as compare to the ball bar result, this equate the straightness error in the XY plane. EYX represents the straightness error of the X-axis in the Y direction.

$$E_{YX} = E_{YX0} + E_{YX1} * x + E_{YX2} * x^2 + E_{YX3} * x^3 + E_{YXb} * x^{+1/-1} \quad 3-1$$

$$E_{YX} = E_{YX2} * x^2 \quad 3-2$$

Where +1/-1 is the direction of motion

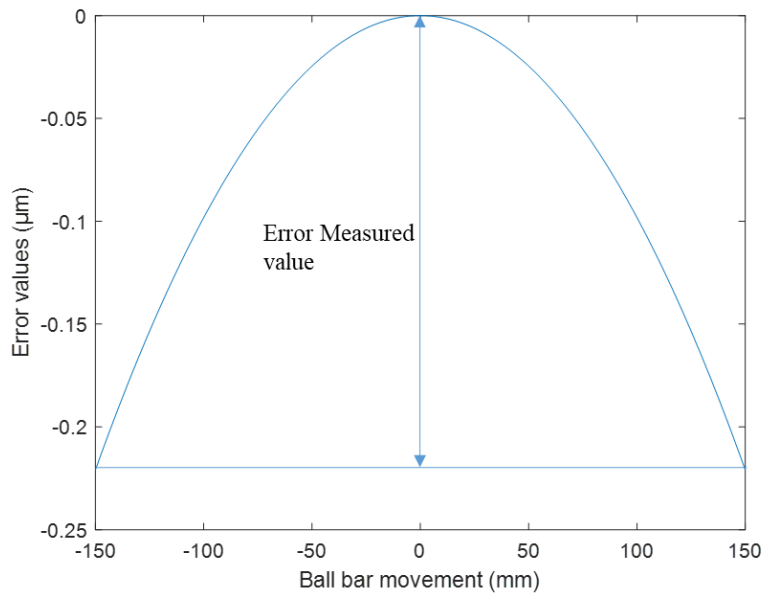


Figure 3.9: Straightness error EYX

It is obtained by the polynomial graph from Equation 3.1 to make it comparable with the ball bar. Polynomial equation's factor from zero degrees to third-degree indicates the error parameter coefficient for error modeling of the five-axis machine tool.

Figure 3.9 shows the straightness error measurement compared with the ball bar. It has CW and CCW movement in each test to measure the error parameter. The Renishaw ball bar software directly provides the value of error, but in the S/T method, it is a polynomial coefficient, and the distance in Figure 3.9 shows the measured value of straightness EYX.

Furthermore, applying the same procedure to obtain other straightness EZX, EXY, EZY, EXY, EYZ.

3.5 Backlash error measurement

In the SAMBA / TANGO method, EXXb and EYYb are the backlash error in x and y-direction, respectively. It is the last polynomial coefficient in Equation 3.3 and 3.4

$$E_{XX} = E_{XX0} + E_{XX1} * x + E_{XX2} * x^2 + E_{XX3} * x^3 + E_{XXb} * x^{+1/-1} \quad 3-3$$

$$E_{YY} = E_{YY0} + E_{YY1} * y + E_{YY2} * y^2 + E_{YY3} * y^3 + E_{YYb} * y^{+1/-1} \quad 3-4$$

While comparing with the Renishaw ball bar, it is a measurement error by the XY test plane in x and y-direction.

3.6 Scaling error measurement

According to the Renishaw ball bar, during experimental work, it is the difference in the measured travels of the axis. The second term of the polynomial equation is equivalent to the scaling error in the ball bar.

$$E_{ZZ} = E_{ZZ0} + E_{ZZ1} * z + E_{ZZ2} * z^2 + E_{ZZ3} * z^3 + E_{ZZb} * z^{+1/-1} \quad 3-5$$

$$E_{XX} = E_{XX1} * x \quad 3-6$$

$$E_{YY} = E_{YY1} * y \quad 3-7$$

There E_{XX1} , E_{ZZ1} , E_{YY1} are the error coefficient in the S/T method to compare the second term with the ball bar it was multiplied by the ball bar circular movement, which is 300 mm in diameter.

The value of x, y, and z took as 300 mm.

The Renishaw software provides the scaling error measurement in ppm (part per million). For comparison with the S/T method, their value was converted to mm. For example

If scaling error in x-axis is, 30ppm and test radius is 150 mm then

$$30 * 10^{-6} * 2 * 150 \text{ mm} = 0.009 \text{ mm}$$

3.7 Squareness error measurement

It is the first term of the polynomial equation to measure squareness error in the S/T method while from Renishaw software, it measured in the XY, YZ, and ZX test plane. Table 3.3 shows the all parameter chosen from the polynomial equation for all axis.

$$E_{CZ} = E_{CZ0} * z^0 + E_{CZ1} * z^1 + E_{CZ2} * z^2 + E_{CZ3} * z^3 + E_{CZb} * z^{+1/-1} \quad 3-8$$

$$E_{CX} = E_{CX0} * x^0 + E_{CX1} * x^1 + E_{CX2} * x^2 + E_{CX3} * x^3 + E_{CXb} * x^{+1/-1} \quad 3-9$$

$$E_{XZ} = E_{XZ0} * z^0 + E_{XZ1} * z^1 + E_{XZ2} * z^2 + E_{XZ3} * z^3 + E_{XZb} * z^{+1/-1} \quad 3-10$$

Table 3.3: Error parameter notation in SAMBA/TANGO and ball bar method

Error Parameter		
SAMBA/TANGO notation		Ball bar notation
1	EXXb	BACKLASH ERROR
2	EYYb	
3	EXYb	LATERAL PLAY ERROR
4	EYXb	
5	EYZb	
6	EZYb	
7	EZXb	
8	EXZb	
9	$EYX = EYX_2 * x^2$	STRAIGHTNESS ERROR
10	$EZX = EZX_2 * x^2$	
11	$EXY = EXY_2 * y^2$	
12	$EZY = EZY_2 * y^2$	
13	$EXZ = EXZ_2 * z^2$	
14	$EYZ = EYZ_2 * z^2$	
15	$EXX = EYX_1 * x$	SCALING ERROR
16	$EYY = EYX_1 * y$	
17	$EZZ = EYX_1 * z$	
18	ECZ0	SQUARENESS ERROR
19	ECX0	
20	EXZ1	

CHAPTER 4 REVERSAL ERROR MEASUREMENT

This section shows the experimental procedure to measure the reversal error of the HU40T machine tool. Six reversal error was measured while probing in X, Y, and Z direction.

4.1 Reversal error measurement including Pre movement

The indexation 17 to 21 in Table 3.1 was developed to acquire the reversal error and backlash error. Only one facet was utilized to estimate the reversal error, pre-motions were used in the X, Y, Z, axis directions.

The reversal error EXYb, EXZb, EZXb, EZYb, EYXb, and EYZb were measured using the pre-movement technique.

According to the Renishaw ball bar software, reversal is a tangential error in the XY, YZ, and ZX test planes. In the S/T method, it was obtained by the last term coefficient of a polynomial equation (see equation 4.1 as an example).

EXYb, EYXb are reversal errors in the XY test, EYZb, EZYb is reversal errors in the YZ test plane, and EZXb, EXZb is reversal errors in the ZX test plane from the Renishaw software.

4.1.1 Reversal Error EXYb and EXZb

EXYb, EXZb is the reversal error in the X-direction. The pre-movement technique in y and z-directions obtained these errors.

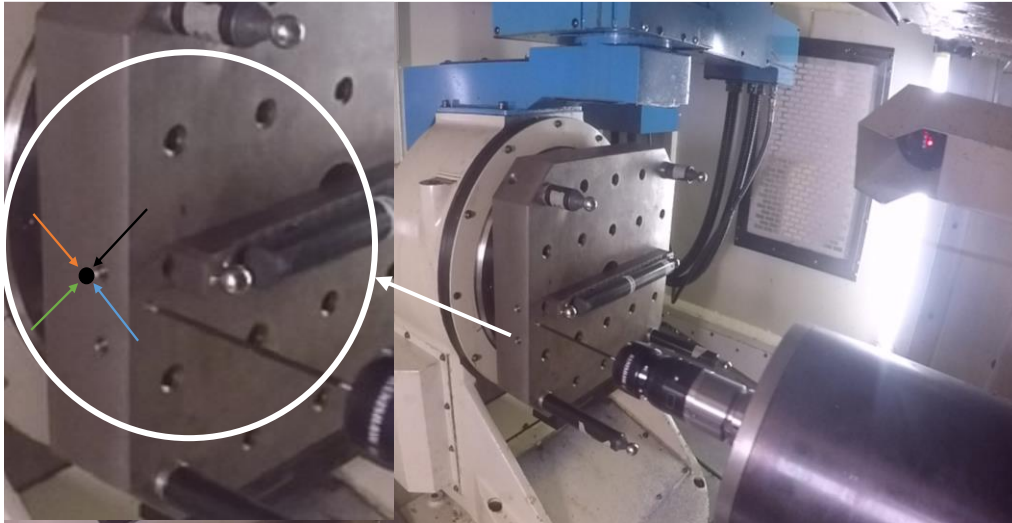
$$E_{XY} = E_{XY0} * y^0 + E_{XY1} * y^1 + E_{XY2} * y^2 + E_{XY3} * y^3 + E_{XYB} * y^{+1/-1} \quad 4-1$$

$$E_{XZ} = E_{XZ0} * z^0 + E_{XZ1} * z^1 + E_{XZ2} * z^2 + E_{XZ3} * z^3 + E_{XZB} * z^{+1/-1} \quad 4-2$$

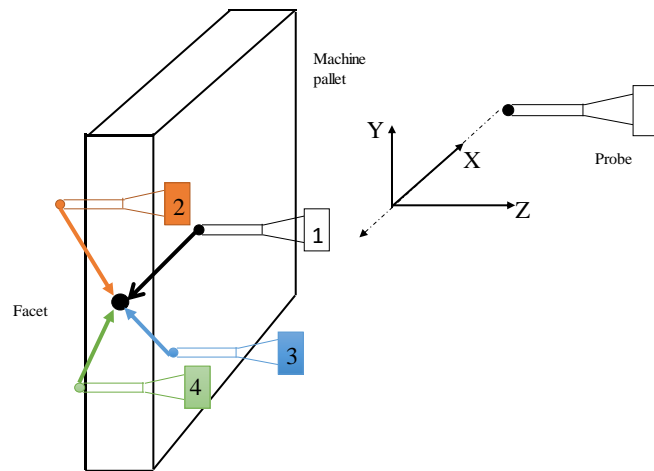
As shown in Figure 4.1(b), the probe is moved in y and z-direction diagonally. The reversal error was measured by using the indexation 17. In the first step, bring the probe to the face and complete the pre-movement.

For the first move, as shown in Figure (4.1,b), the probe moves in y and z positive direction diagonally then again back move in negative y and z-direction this complete the first pre-movement. After both moves, probe the face in the x-direction for reversal error measurement.

In the second pre-move, as shown in Figure (4.1,b), the probe moves forward in y positive and z negative direction, then moves backward in y negative and z positive after completing this process probe the same face in the x-direction to get reversal error data.



(a)



(b)

Figure 4.1: Probing movement reversal error EXYb and EXZ

The third movement has a backward movement in y negative and z positive direction than forwarding movement in y positive and z negative direction. Likewise, the fourth move in negative y and z-direction and move back in positive y and z-direction. Finally, the probe in the X direction by moving the machine pallet.

Table 4.1: Reversal error Pre-movement direction

Error parameter measured	Pre-movement direction			
	Pre-move	X	Y	Z
EXYb and EXZb	First	Probing Direction	-1	-1
	Second		-1	+1
	Third		+1	-1
	Fourth		+1	+1
EZXb and EZYb	First	-1	-1	Probing Direction
	Second	+1	-1	
	Third	+1	+1	
	Fourth	-1	+1	
EYXb and EYZb	First	-1	Probing Direction	-1
	Second	-1		+1
	Third	+1		+1
	Fourth	+1		-1

Table 4.1 shows the probing movement with its negative and positive direction, as developed for the new approach to measuring the reversal error and backlash error.

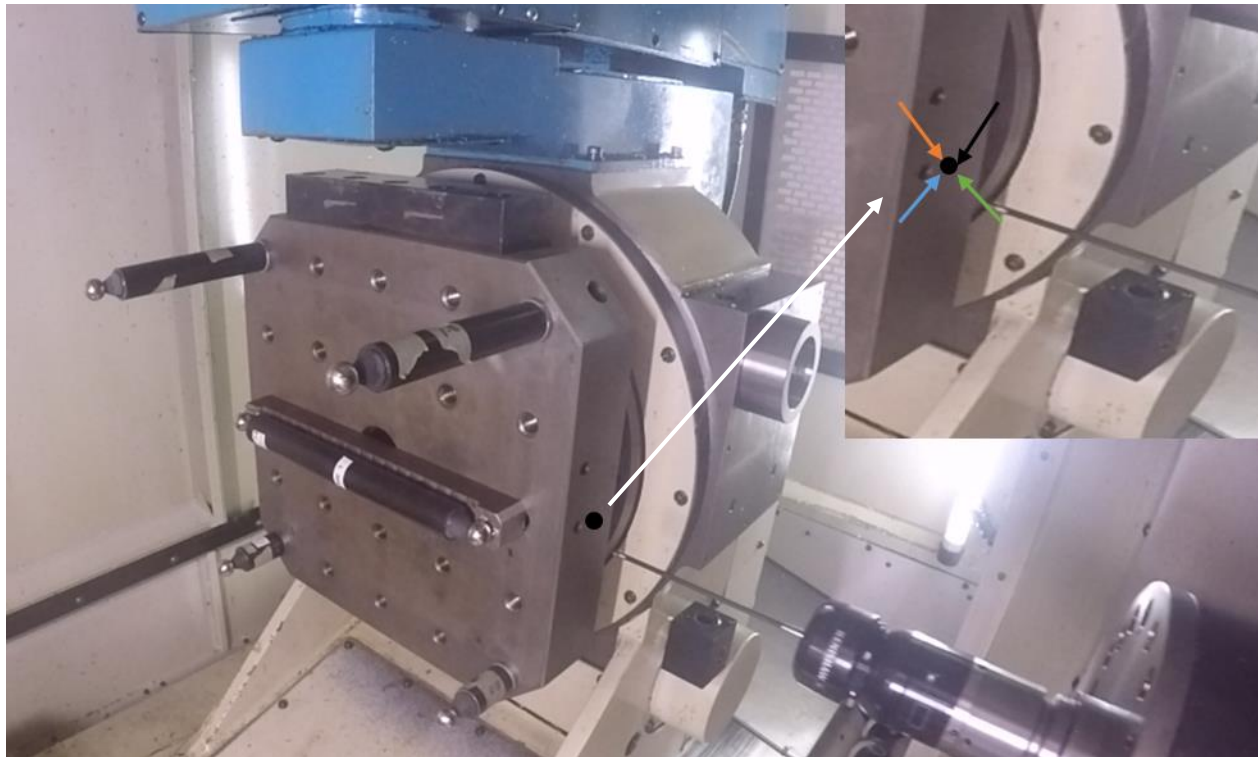
4.1.2 Reversal Error EZXb and EZYb

EZXb and EZYb is the reversal error in the z-direction. As shown in Figure 4.2 (a, b), these are measured by the diagonal pre-movement in x and y-directions. The errors are analyzed through probing in the z-direction, according to indexation 18, shown in Table 3.1. The procedure is the same as the previous reversal error, but their direction is changed, as illustrated in Figure 4.2 for the pre-move.

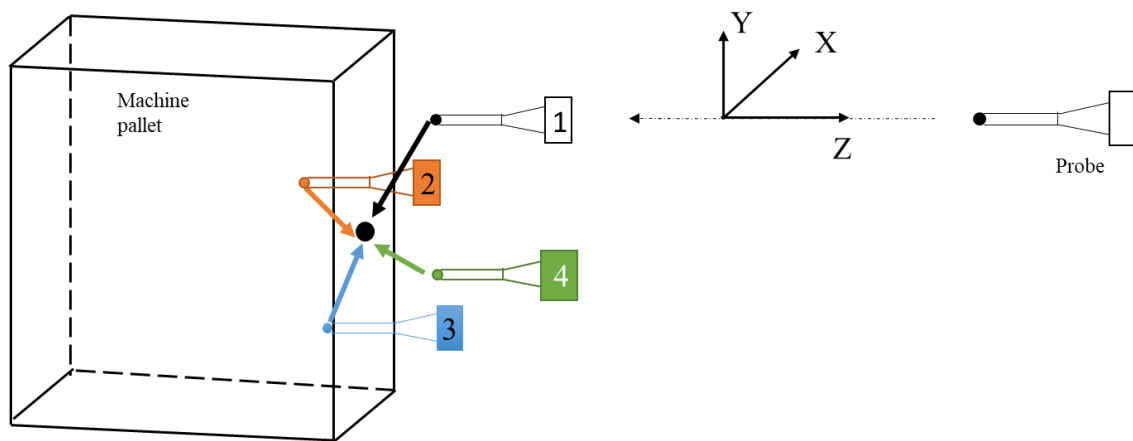
$$E_{ZY} = E_{ZY0} * y^0 + E_{ZY1} * y^1 + E_{ZY2} * y^2 + E_{ZY3} * y^3 + E_{ZYB} * y^{+1/-1} \quad 4-3$$

$$E_{ZX} = E_{ZX0} * x^0 + E_{ZX1} * x^1 + E_{ZX2} * x^2 + E_{ZX3} * x^3 + E_{ZXB} * x^{+1/-1} \quad 4-4$$

Where z is the direction of error. X and Y is the leading axis movement.



(a)



(b)

Figure 4.2: Probing movement reversal error $EZXb$ and $EZYb$

4.1.3 Reversal Error $EYXb$ and $EYZb$

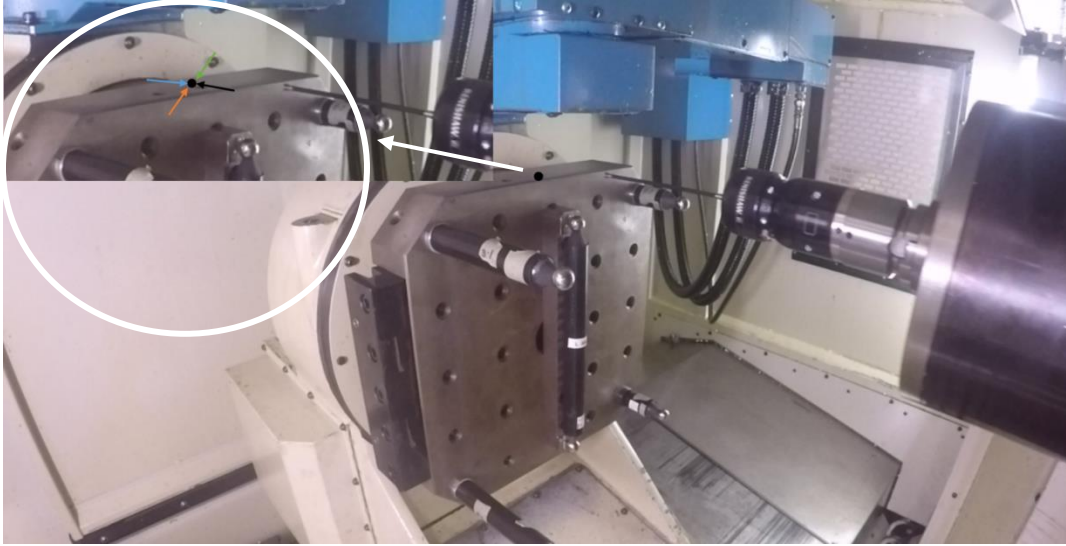
$EYXb$ and $EYZb$ is reversal error in the y-direction. These errors gained by the pre-movement in x and z direction diagonally, as shown in Figure 4.3. In these error parameters, the direction of the error is y, and the main axis movement is in x and z-direction. Error-values analyzed by employing

the indexation 19 from Table 3.1. The Probe movement path is the same as other reversal errors, but their direction of the moving axis was changed, as shown in Figure 4.3.

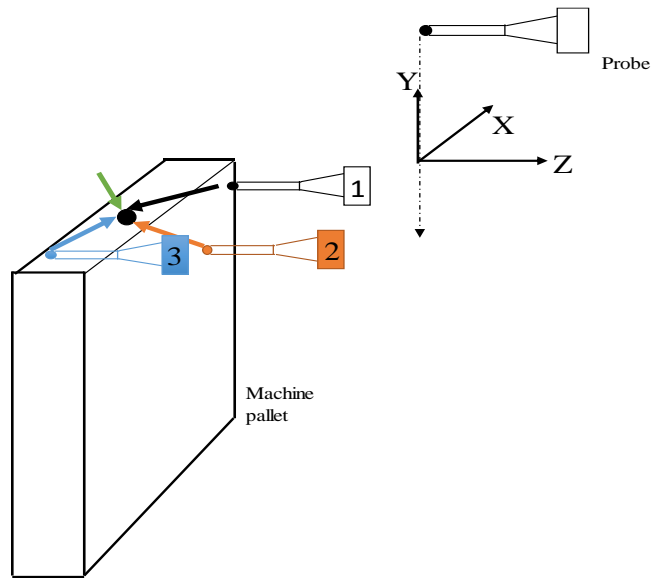
$$E_{YX} = E_{YX0} * x^0 + E_{YX1} * x^1 + E_{YX2} * x^2 + E_{YX3} * x^3 + E_{YXB} * x^{+1/-1} \quad 4-5$$

$$E_{YZ} = E_{YZ0} * z^0 + E_{YZ1} * z^1 + E_{YZ2} * z^2 + E_{YZ3} * z^3 + E_{YZB} * z^{+1/-1} \quad 4-6$$

It has four pre-movement before each probing.



(a)



(b)

Figure 4.3: Reversal error EYXb and EYZb

Table 4.2: Mean error and standard measured values by BB and by S/T method

Error Parameter			Ballbar		SAMBA/TANGO		Range
			Average	Stdev.	Average	Stdev.	
1	EXXB	BACKLASH (μm)	-0.81	0.28	-2.39	4.87	1.58
2	EYYB		2.64	0.37	-12.58	3.79	15.21
3	EXYB	LATERAL PLAY (μm)	0.07	0.29	0.37	0.73	0.30
4	EYXB		0.94	0.29	0.22	0.87	0.72
5	EYZB		0.23	0.13	-0.03	1.00	0.25
6	EZYB		-0.19	0.29	0.38	0.32	0.57
7	EZXB		-0.48	0.13	0.13	0.32	0.60
8	EXZB		-0.255	0.16	0.13	0.51	0.39
9	EYX	STRAIGHTNESS (μm)	-0.11	0.40	-0.22	0.08	0.11
10	EZX		-0.48	0.20	-4.22	0.33	3.74
11	EXY		2.08	0.22	0.67	0.18	1.40
12	EZY		-0.71	0.26	1.76	0.24	2.47
13	EXZ		-3.11	0.37	1.05	0.33	4.16
14	EYZ		2.09	0.27	0.48	0.09	1.61
15	EXX	SCALING (μm)	-4.65	4.81	-4.67	0.50	0.03
16	EYY		2.50	5.36	0.03	1.26	2.48
17	EZZ		-1.31	4.57	2.26	0.84	3.57
18	ECZ0	SQUARNESS ($\mu\text{m}/\text{m}$)	7.26	3.26	19.74	2.22	12.48
19	ECX0		18.68	1.26	-1.17	0.97	19.85
20	EXZ1		-6.48	1.64	-37.04	11.03	30.56

Table 4.2 shows the experimental and analyzed data from the Renishaw and S/T software. Standard deviation is also analyzed in Table 4.2 and graphically presented in section 5.1. An absolute difference also presented in Table 4.2.

CHAPTER 5 RESULT ANALYSIS

The experimental data and graphical representation were explained in this chapter. Chapter 5 includes two sections one is error analysis, and the second section concerns the correlation between the BB and S/T error parameters.

5.1 Error analysis

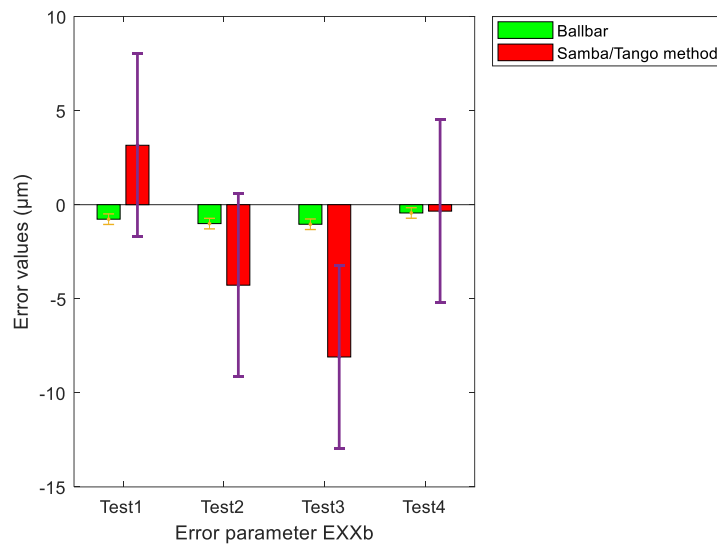
5.1.1 Backlash error in the X direction (EXXb)

The Renishaw software analyses the EXXb error in the X direction for the plan XY and ZX. To estimate the same error parameter with the S/T method, it is the last term in the polynomial Equation 3.3.

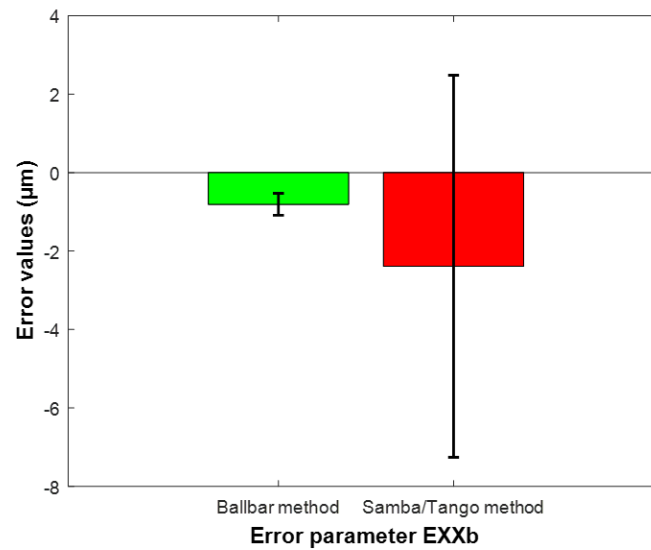
Figure 5.1(a) shows that the ball bar measured data always have negative error values and the S/T estimated error value for test 1 is positive, and for the rest of the test, these values are negative, but test 4 indicates the same measured value in both methods.

The graphical representation of the mean error value illustrated in Figure 5.1(b). The ball bar measured mean error value is $-0.81 \mu\text{m}$ and $-2.39 \mu\text{m}$ by the S/T method. Their absolute difference is $1.58 \mu\text{m}$.

When considering the standard deviation bands, the values overlap, meaning that the results can be considered in close agreement and conclude that the EXXb error parameter is associated with both methods.



(a)

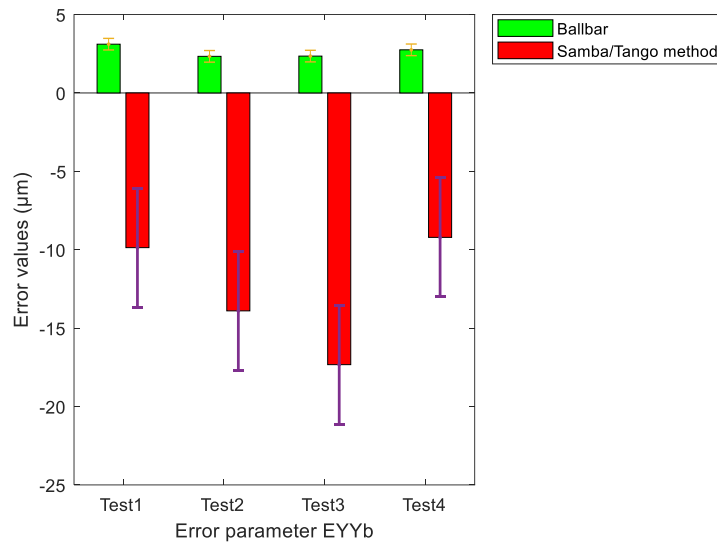


(b)

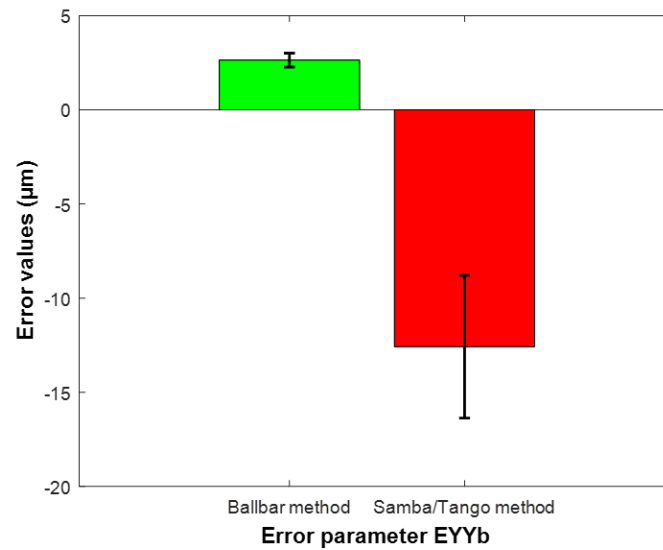
Figure 5.1: Error Parameter EXXb

5.1.2 Backlash error in the Y direction (EYYb)

EYY is the last order term in the polynomial Equation 3.4 to measure the backlash in the Y direction, and for the Renishaw ball bar software EYYb is the XY, YZ plan error in the y-direction



(a)



(b)

Figure 5.2: Error Parameter EYYb

The result of both methods for parameter EXXB were presented, as shown in Figure 5.2. They have entirely different error values; the ball bar measured values are positive and quite close to each other; oppositely, to the second method, backlash error values are negative.

Figure 5.2 (b) shows that the average error values of the ball bar are higher compared to the S/T method. Backlash error in the y-direction by the Renishaw software is 2.64 μm , and S/T measured

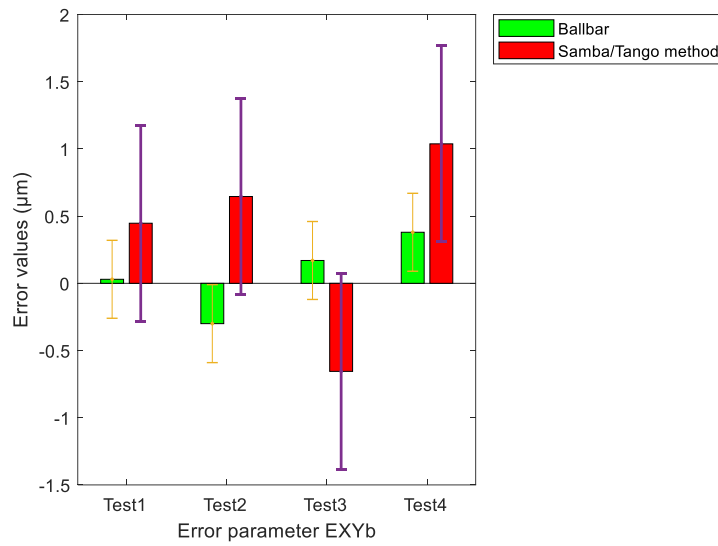
error is $-12.58 \mu\text{m}$. The absolute difference is $15.21 \mu\text{m}$. It has a second-highest difference in all compared geometric error parameters.

5.1.3 Reversal Error (EXYb)

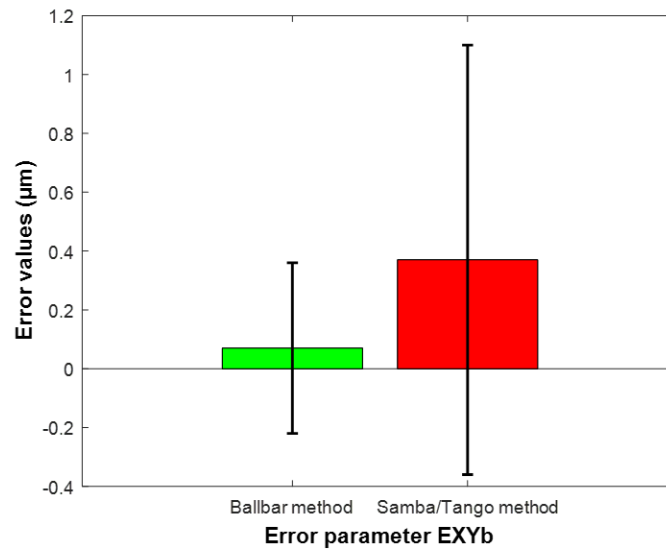
The lateral play error EXYb is obtained by the XY plane test from the Renishaw software, and it is the last term of polynomial Equation 4.1 in the S/T technique.

Figure 5.3 shows that test 1 and test 4 have the same positive trend of measured error, but in test 2 and test 3, error values are in the opposite sign for both methods. It can notice that the test1, test 2, have positive error values in both methods.

The mean error value from Figure 5.3(b) is $0.07 \mu\text{m}$ by ball bar analysis and $0.37 \mu\text{m}$ for the S/T method. Their absolute difference is $0.30 \mu\text{m}$. The results overlap within the standard deviation zone, and the absolute difference is also less, shows that error parameter values are in close agreement.



(a)



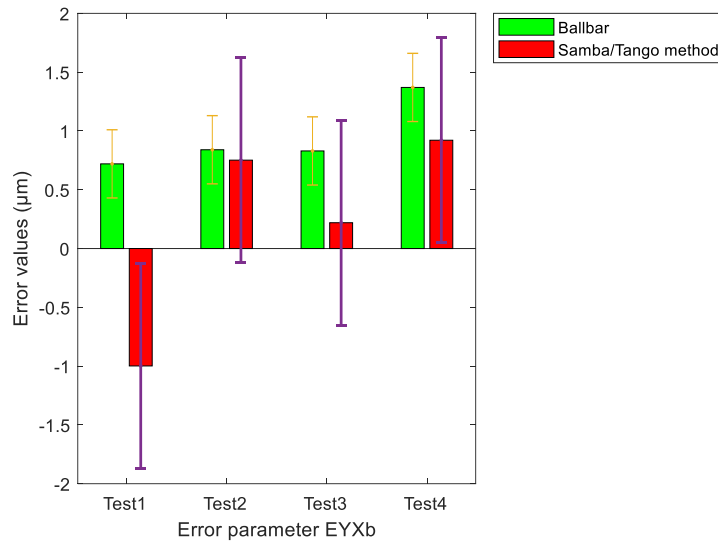
(b)

Figure 5.3: Error Parameter EXYb

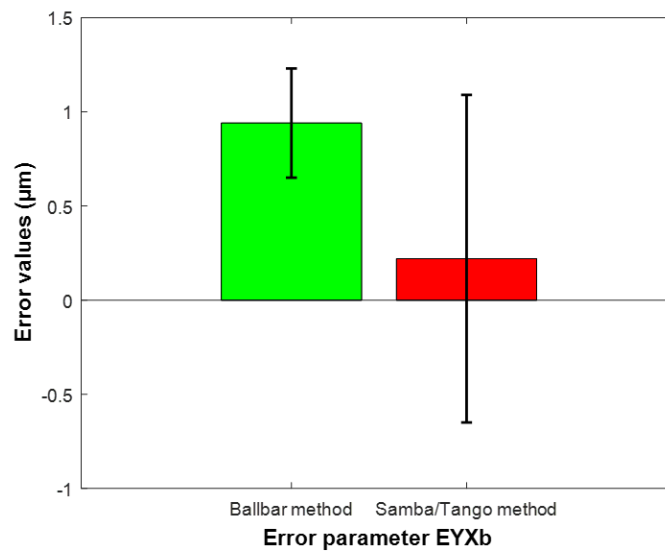
5.1.4 Reversal Error (EYXb)

EYXb is the lateral play error for the X-axis in the Y-direction as per the Renishaw software. To estimate with the S/T method, the parameter selected from the polynomial equation is the last term in Equation 4.5.

Figure 5.4 (a) shows the graphical representation of analyzed data by the ball bar and S/T technique. All initial three-test for ball bar measured values are similar, but the last test increased by 1 μm . On the other hand, in the first test, the S/T method value measured is negative, and then for all other tests, it extended positively.



(a)



(b)

Figure 5.4: Error Parameter EYXb

The mean error values are illustrated in Figure 5.4(b). The mean error value of all four tests is $0.94\ \mu\text{m}$ in ball bar estimation and $0.22\ \mu\text{m}$ by the S/T technique. The difference between these two methods for EYXb is $0.72\ \mu\text{m}$, and the standard deviation region does not overlap but only by $0.58\ \mu\text{m}$. It can consider a lean error parameter in comparison.

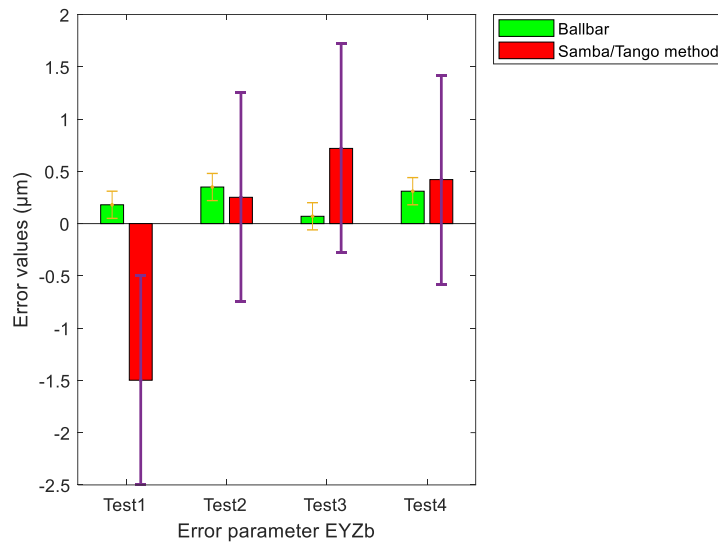
5.1.5 Reversal Error (EYZb)

EYZb is the reversal error when probing in the y-direction and the axis movement is in the z-direction. EYZb has selected the last term from Equation 4.6 in S/T method. The Renishaw ball bar refers to it as a lateral play error in the YZ plane for the y-direction movement.

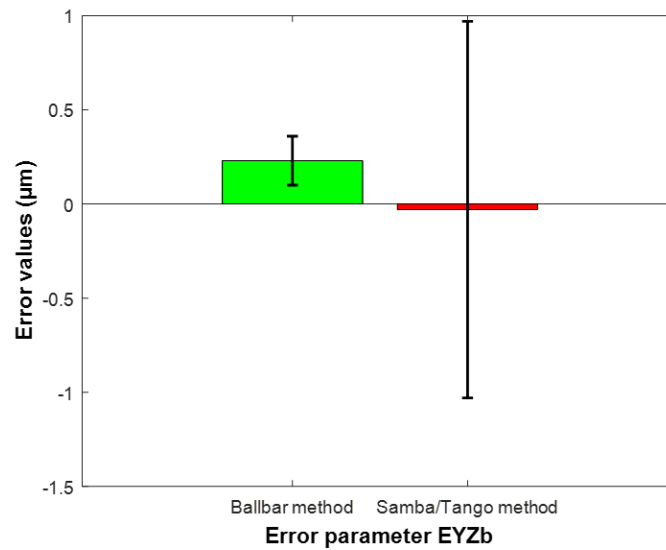
The ball bar method measured error values are presented in Figure 5.5(a), and it shows that all test data for the ball bar are positive. The S/T method measured values are also in a positive trend, but the first test shows a negative error value.

It is noted in Figure 5.5(b) that the error bar in the S/T method compares to the ball bar is more extensive; the results for the two methods overlap in standard deviation, and parameter EYZb is associated with both methods.

The analyzed mean error parameter is $0.23\ \mu\text{m}$, as noted in the ball bar method and $-0.03\ \mu\text{m}$ for the S/T method. The absolute difference for this parameter is $0.25\ \mu\text{m}$, illustrated in Figure 5.5(b). It clearly shows that the standard deviation zone in overlap condition for the EYZb error parameter and consider as in close agreement for both methods.



(a)

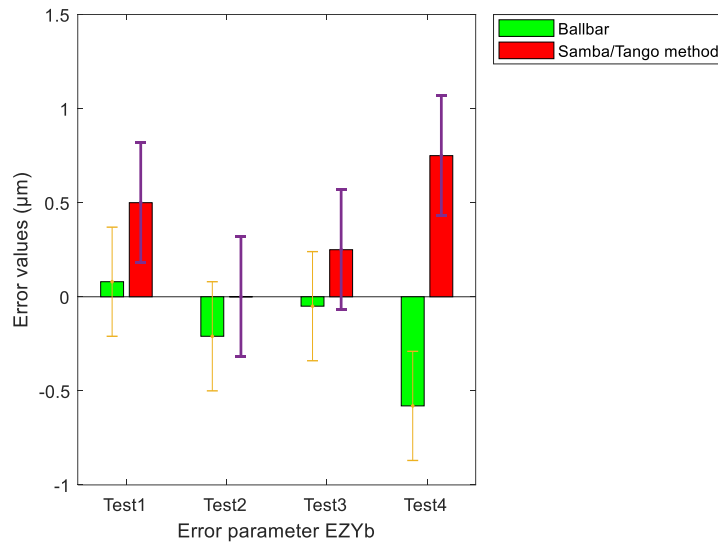


(b)

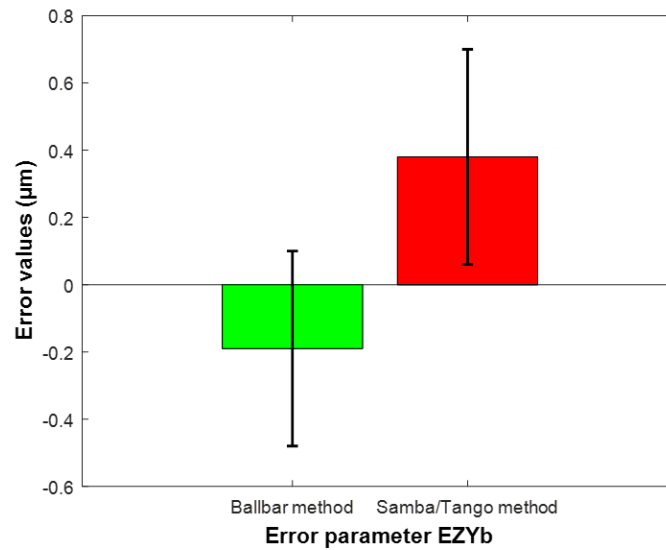
Figure 5.5: Error Parameter EYZb

5.1.6 Reversal Error (EZYb)

From the Renishaw ball bar software, EZYb is a lateral play error in the z-direction of the X-axis. Likewise, it is the last term of polynomial Equation 4.3 for the S/T method.



(a)



(b)

Figure 5.6: Error Parameter EZYb

Figure 5.6(a) (b) shows the trend of analyzed experiment data for the ball bar and S/T method. The Ball bar observed data has negative and positive error values, and the S/T method measured error values were all positive. The standard deviation of Ball bar observation is $0.29 \mu\text{m}$. Figure 5.6 (b) reveals the Ball bar mean error $-0.19 \mu\text{m}$, which is just opposite to the S/T error value of $0.38 \mu\text{m}$.

The different is $0.57\text{ }\mu\text{m}$. The standard deviation region was not overlapped as clear from Figure 5.6, and it is not in acceptable agreement for the comparison purpose.

It is suggested that there may be a negative and positive significant difference in the definition of the reversal error of the BB and S/T method.

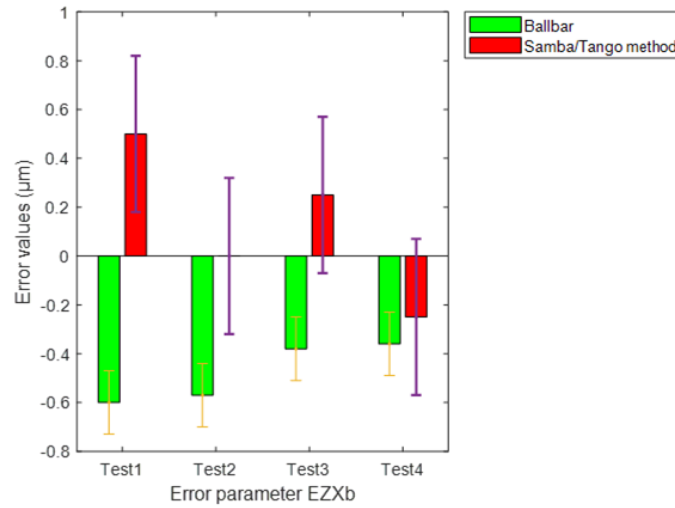
5.1.7 Reversal Error (EZXB)

EZXB is lateral play errors in ZX plane from the Renishaw software in Z -direction. Whereas for the S/T method, it is the last term of polynomial 4.4.

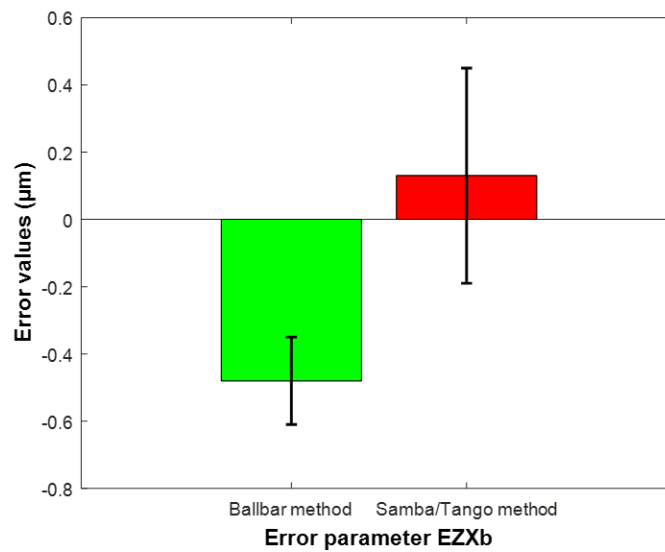
Figure 5.7 (a) shows the measured error value graph for both methods. The ball bar estimated error values have the same trend, and all values are negative. On the other hand, the S/T method has dramatically changed in test 1, 3 shows negative value, and test 2 has negligible value.

EZXB gained data by the ball bar is $-0.48\text{ }\mu\text{m}$ and $0.13\text{ }\mu\text{m}$ for the S/T method while their absolute difference is $0.60\text{ }\mu\text{m}$. The standard deviation region does not overlap, as shown in Figure 5.7. The ball bar value is small compared to the S/T measured value.

EZXB error parameter does not show any agreement for both methods.



(a)

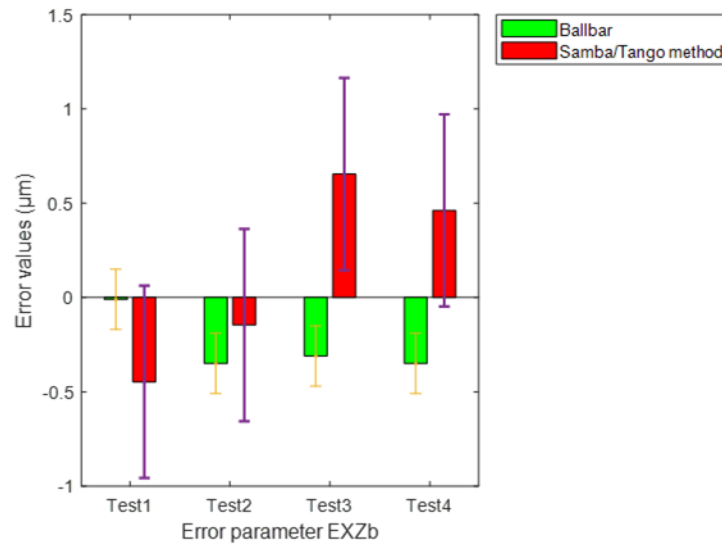


(b)

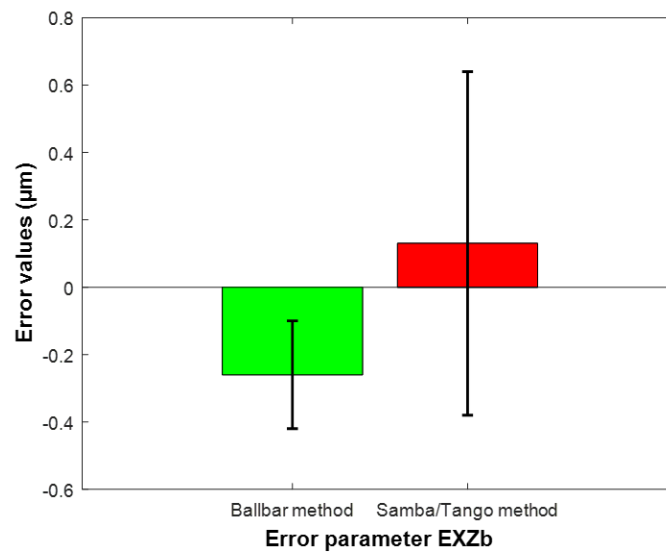
Figure 5.7: Error Parameter EZXb

5.1.8 Reversal Error (EXZb)

EXZb is lateral play errors in ZX plane from the Renishaw software in X -direction. Whereas for the S/T method, it is the last term of polynomial 4.2. As illustrated in Figure 5.8 (a), ball bar test 1 data is negligible, and another test value is negative in a similar trend. Test 1 and test 2 have negative value, while test 3 and test 4 measured positive value in the S/T method.



(a)



(b)

Figure 5.8: Error Parameter EXZb

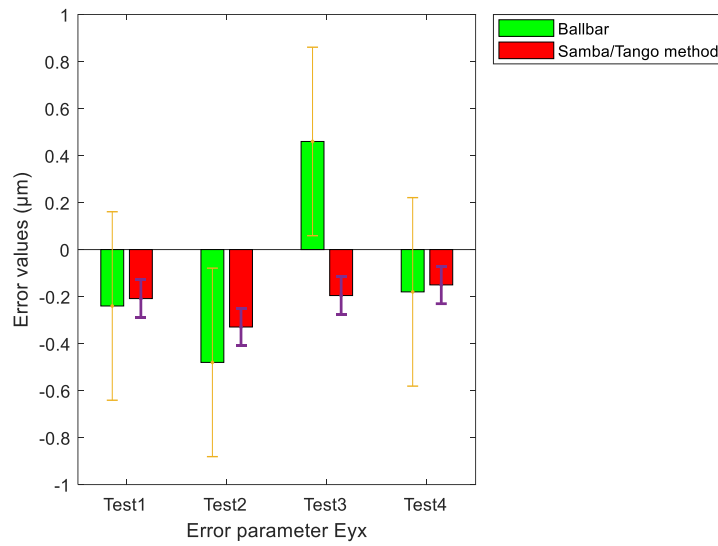
As obtained by the Renishaw software EXZb is $-0.26 \mu\text{m}$ and the S/T method value is $0.13 \mu\text{m}$. Consequently, their difference is $0.39 \mu\text{m}$. Instead of different error values, their standard deviation region overlap, but technically EXZb is not considered for the close agreement.

5.1.9 Straightness error of X-axis in Y direction (EYX)

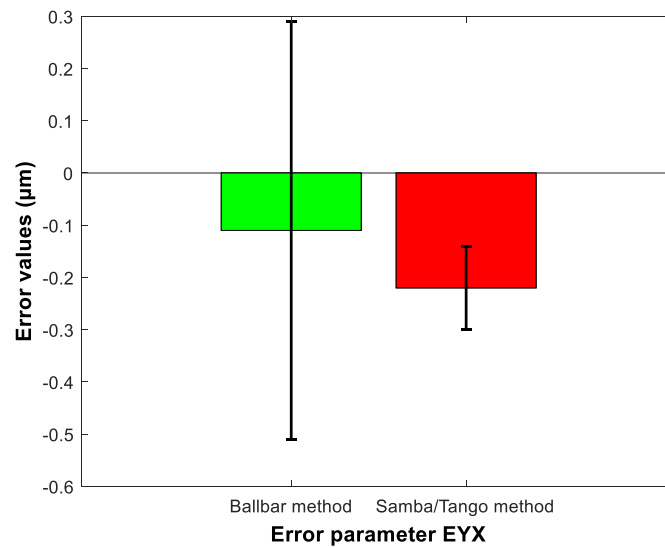
Figure 5.9 (a) shows the four days repeated the test with the same condition. Figure 5.9(b) represents the bar chart between mean error values and the EYX error parameter for both SAMBA and Ball bar method.

EYX is the straightness error of the X-axis in the Y direction. It is clear from Figure 5.9(b) that the measured error values for all four consecutive days are similar for both methods. All values have minus signs for the ball bar, and the third-day value is not the same as others. The error value suddenly goes from negative to positive.

The mean error value of EYXb is $-0.11 \mu\text{m}$ and $-0.22 \mu\text{m}$ for the SAMBA and Ball bar method, respectively. The absolute difference is $0.08 \mu\text{m}$. From figure 5.9(b), the standard deviation overlap; consequently, the error values are in close agreement.



(a)



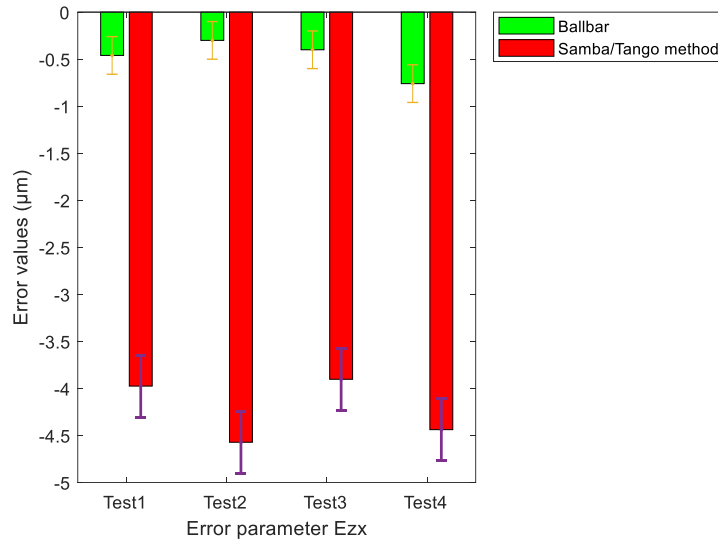
(b)

Figure 5.9: Representation of error parameter EYX

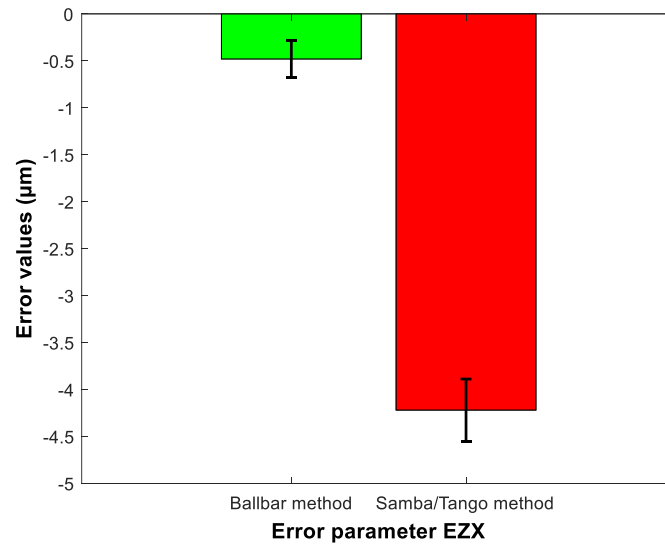
5.1.10 Straightness error of X-axis in the Z direction (EZ_X)

This error parameter is gain from the second order of polynomial Equation 4.4 in the S/T method. As well as, in the Renishaw ball bar software, this is straightness in the XY plane.

The ball bar estimated values are in the same trend and close to each other, as clear from Figure 5.10 (a). The S/T method value also shows a similar pattern for obtained value, but in both methods, the values have more differences.



(a)



(b)

Figure 5.10: Representation of error parameter EZX

It can be observed in Figure 5.10 (a) that straightness in the Z direction for both observed data is negative. The ball bar value is much smaller than the SAMBA/TANGO error value. The absolute

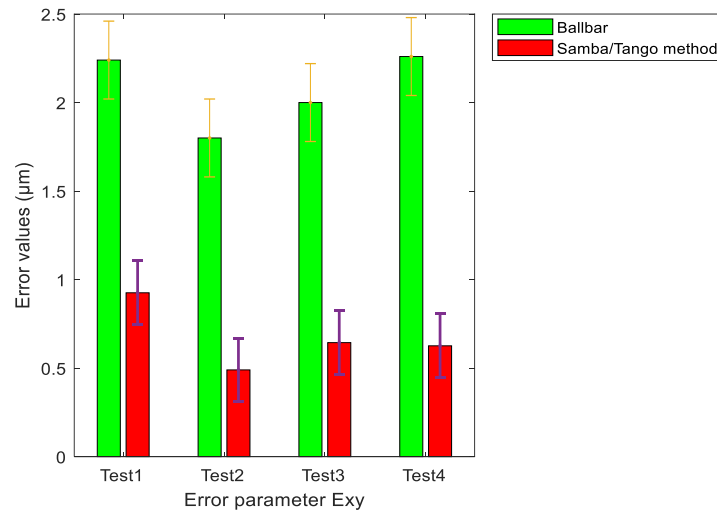
difference is $3.74\text{ }\mu\text{m}$, which is far higher than the standard deviation of both methods. EZX cannot agree in this study. From the analyzed experimental data, the Ball bar error value is $-0.48\text{ }\mu\text{m}$, and the S/T method value is $-4.22\text{ }\mu\text{m}$. In both techniques, the standard deviations are relatively small. The standard deviation region is far away from each other.

5.1.11 Straightness error of Y-axis in the X direction (EXY)

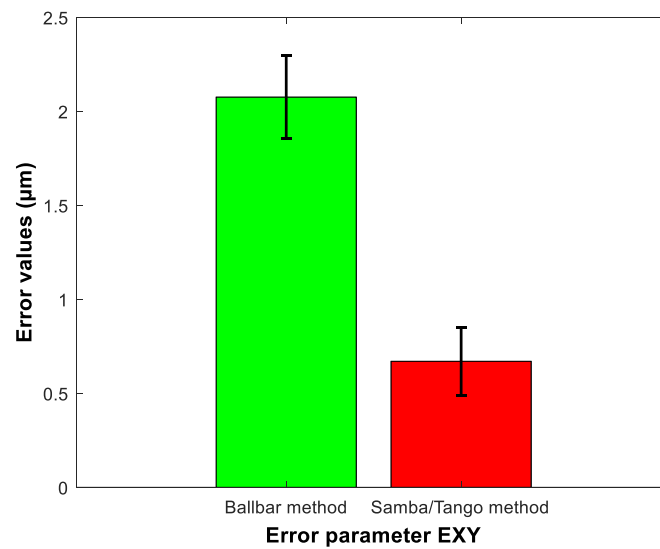
EXY is the error parameter from the Renishaw ball bar software in the YZ plane and the second-order term of polynomial Equation 4.1 in the S/T method.

Figure 5.11 (a) shows the same pattern for the S/T measured error value, and ball bar error values are in a similar trend. Both methods have positive error values, but the ball bar measured error values are higher in all tests compared to the S/T method.

The error discrepancies can be visual in Figure 5.11 (a) for both methods. The estimated average error value of the ball bar is $2.08\text{ }\mu\text{m}$, and the S/T value is $0.22\text{ }\mu\text{m}$. Their absolute difference is $1.40\text{ }\mu\text{m}$. The standard deviation does not overlap, and the BB standard deviation is higher than the S/T standard deviation. EXY parameter is not possible to agree in this study.



(a)

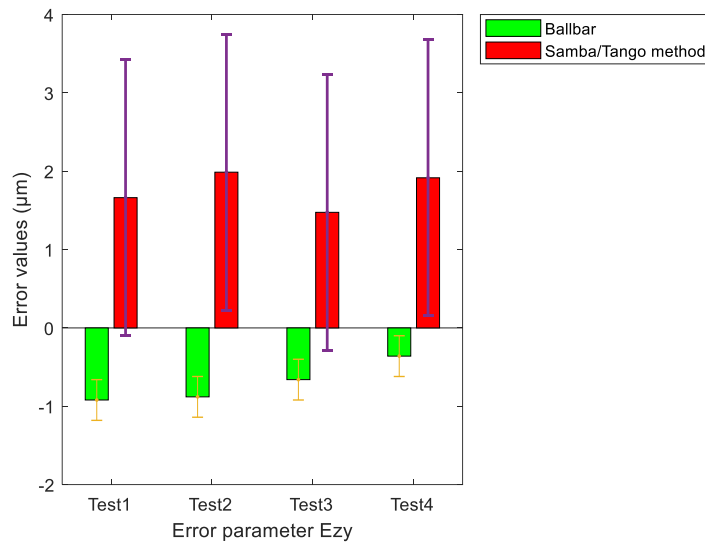


(b)

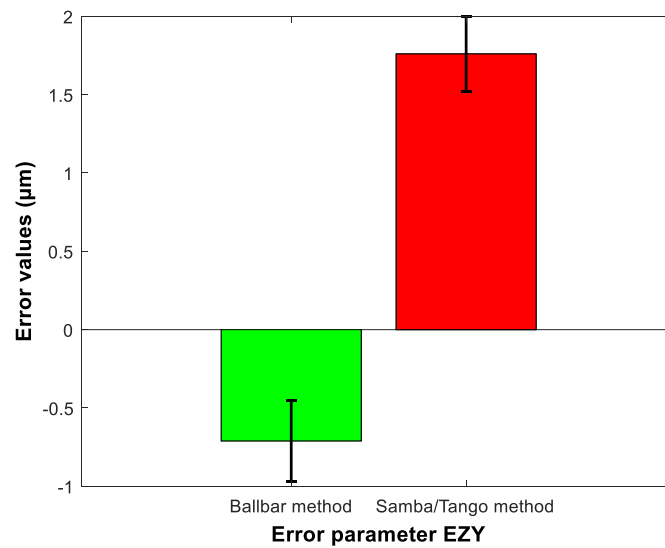
Figure 5.11: Representation of error parameter EXY

5.1.12 Straightness error of Y-axis in the Z direction (EZY)

For EZY, the direction of the error is in the z-direction and the leading axis movement in the y-direction. It was the second-order term from the polynomial Equation 4.3 in the S/T method. On the other hand, from the Renishaw ball bar, EZY is a YZ plane error in the Z direction.



(a)



(b)

Figure 5.12: Representation of error parameter EZY

It is visible from Figure 5.12 (a) that the ball bar experiment data is negative for entirely four experiments, whereas the S/T method data shows the positive value for the all-consecutive experiment.

The mean error value for the ball bar is $-0.71 \mu\text{m}$ and $1.76 \mu\text{m}$ for the S/T method. The absolute difference is $2.47 \mu\text{m}$.

The EZY error values do not overlap within the standard deviation, and the absolute difference is much higher than the standard deviation of both methods. EZY does not show any relevant agreement.

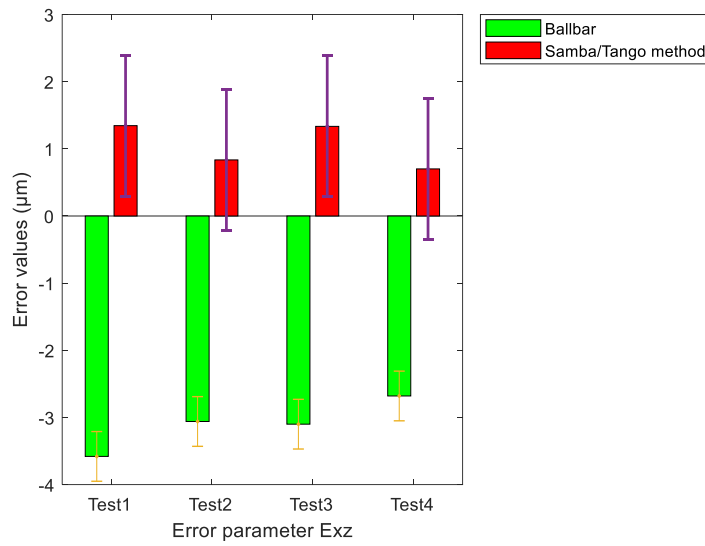
5.1.13 Straightness error of Z-axis in the X direction (EXZ)

The straightness EXZ is the second-order term from Equation 4.2 for the S/T method. As given by the Renishaw ball bar software, this is referred to as straightness error in the ZX plane.

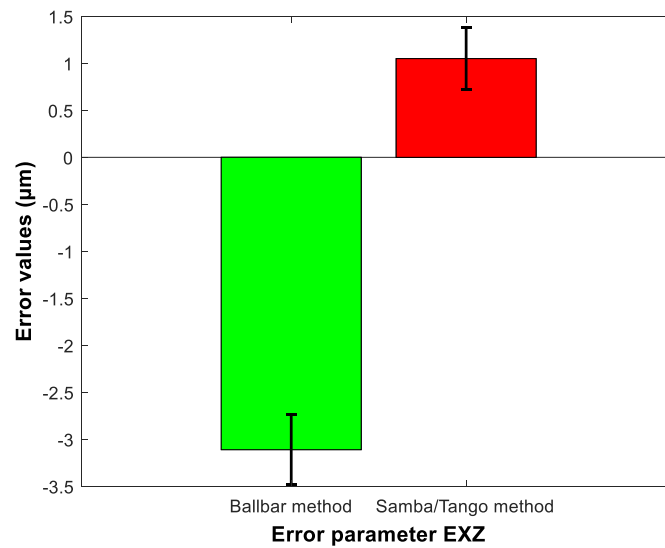
Figure 5.13 (a) shows that the ball bar estimated values are negative for all tests, while for the S/T method, error values are positive for all tests.

The error value from the ball bar very less compared to the S/T method. Figure 5.13 (b) illustrates that the mean error value is $-3.11\ \mu\text{m}$ for the ball bar and $1.05\ \mu\text{m}$ by the S/T method.

The absolute difference is $4.16\ \mu\text{m}$, which is the highest difference in straightness error compare to other straightness. The standard deviation of both methods does not overlap, meaning that these error values are not in agreement.



(a)



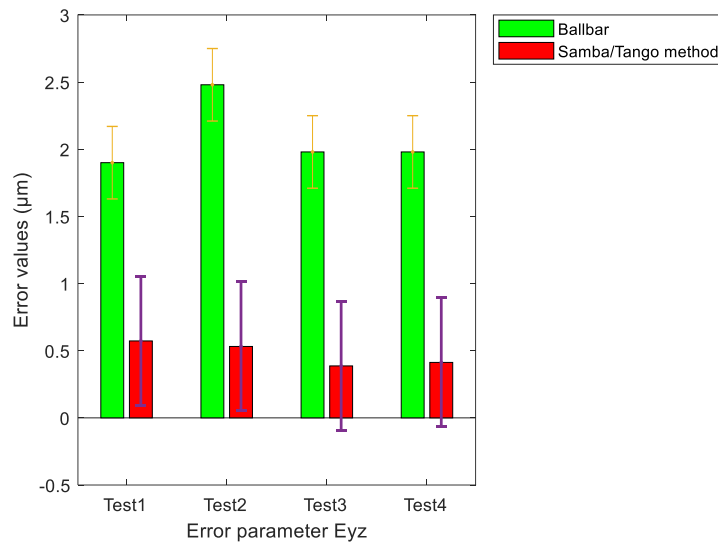
(b)

Figure 5.13: Representation of error parameter EX_Z

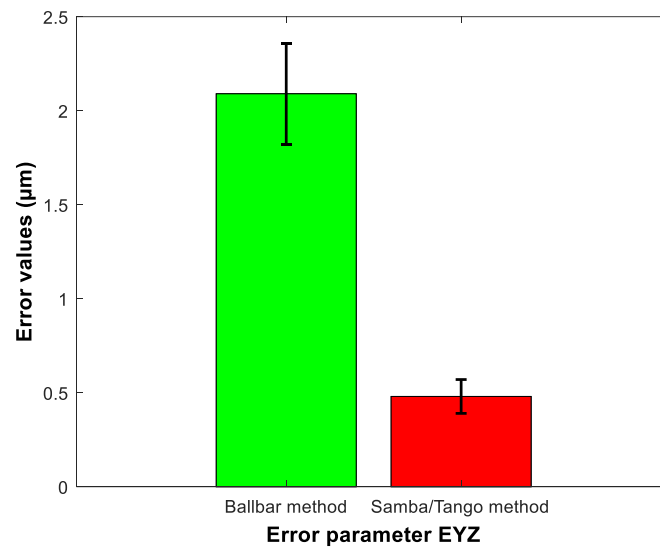
5.1.14 Straightness error of Z-axis in the Y direction (EYZ)

From the Renishaw ball bar software, EYZ is the straightness error in the ZX plane. In the S/T method, this is a second-order term from polynomial Equation 4.6.

Figure 5.14 (a) reveals that the ball bar error value is higher for all tests, while the SAMBA/TANGO method error value is very less.



(a)



(b)

Figure 5.14: Representation of error parameter EYZ

The mean error value for the ball bar analyzed data is $2.09 \mu\text{m}$ and $0.48 \mu\text{m}$ by the S/T method. The difference is $1.61 \mu\text{m}$. It is the fourth highest absolute difference for straightness error.

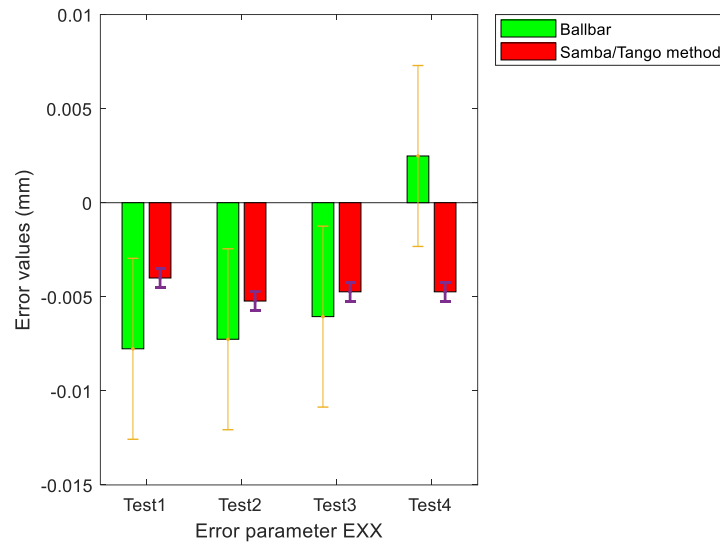
As their difference is immense, the standard deviation does not overlap for EYZ. The error values are not associated with both methods.

5.1.15 Linear positioning error motion of X-axis (EXX)

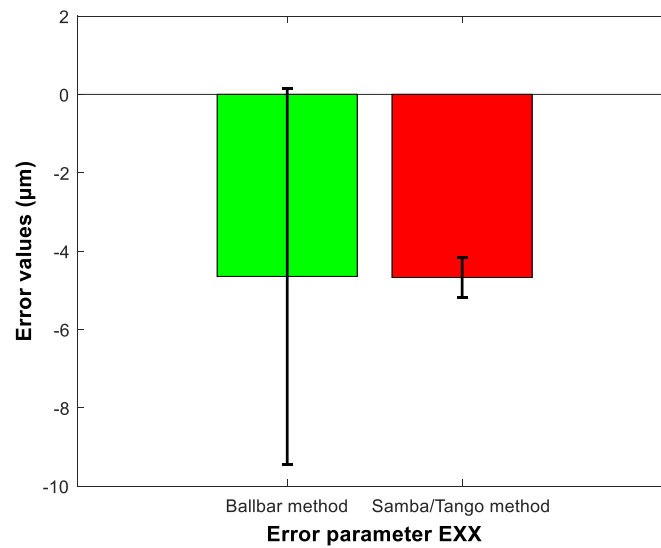
In the ball bar method, EXX is the linear positioning error in XY and ZX plane in the X-direction. It is the first-order term in polynomial Equation 3.3 for the S/T method.

The ball bar experiment data is shown in Figure 5.15 (a) for the first 3 test the ball bar measured negative error values, but for test 4, it jumped to the positive value. While in the SAMBA process, all values are negative.

The ball bar means error from Figure 5.15 (b) is $-4.65 \mu\text{m}$, and the measure means value for the S/T method is $-4.67 \mu\text{m}$. Both measured values are quite similar to each other. Now it can say that this is the most associated error parameter in these methods.



(a)



(b)

Figure 5.15: Representation of error parameter EXX

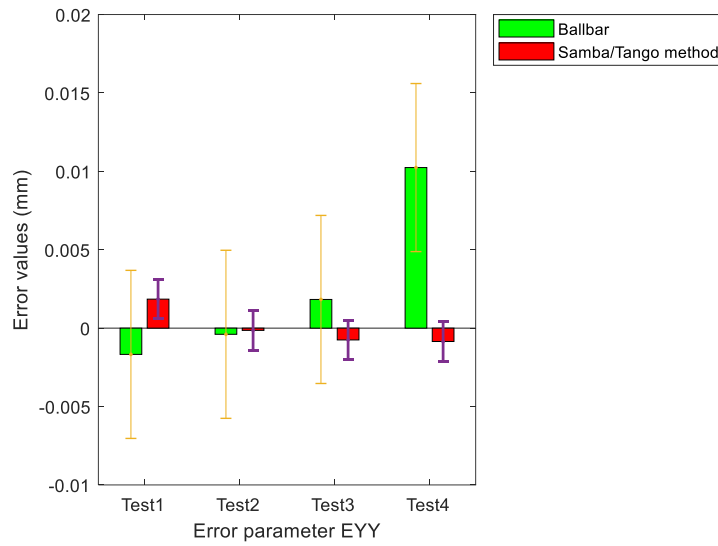
As the absolute difference is $0.03 \mu\text{m}$, the standard deviation overlap for both method and EXX values are in very close agreement. The EXX error parameter was most comparable in the current study.

5.1.16 Linear positioning error motion of Y-axis (EYY)

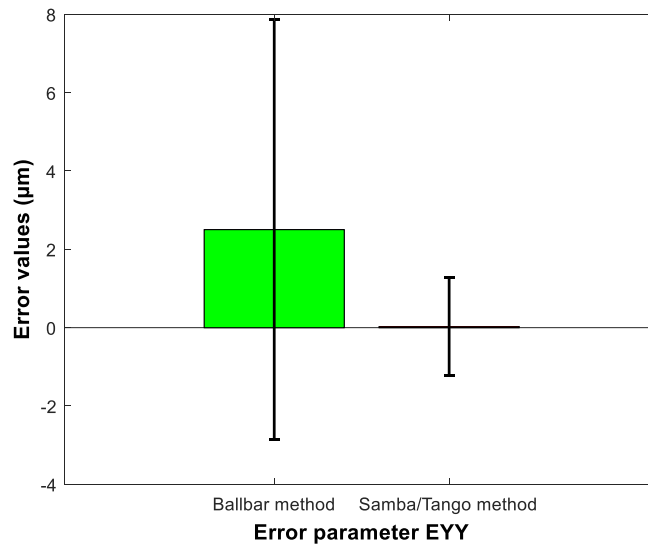
EYY is the linear positioning error from the Renishaw software in YZ and XY plane for the Y direction. For the S/T method, it is the first-order term of Equation 3.4.

The ball bar observed data is not in a similar trend, as it shows in Figure 5.16 (a); it has both negative and positive values. The S/T experimental values are negligible compared to the ball bar.

The analyzed mean error value by the ball bar is $2.5\text{ }\mu\text{m}$. The S/T technique means the error value is $0.03\text{ }\mu\text{m}$, and their difference is $2.48\text{ }\mu\text{m}$, which is equal to the ball bar value. The standard deviation is overlap for both methods.



(a)



(b)

Figure 5.16: Representation of error parameter EYY

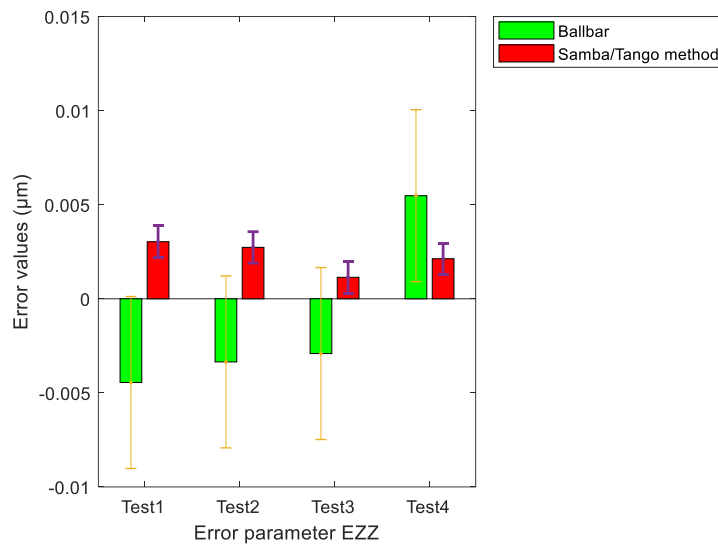
The reason for less value measured by the S/T method might be that the scale bar is measured only in the X-direction. Conditionally measure the scale bar in Y direction such as indexation $A=0$, $B=90$, $C=0$, then it is possible to obtain some comparable value by the S/T method.

5.1.17 Linear positioning error motion of Z-axis (EZZ)

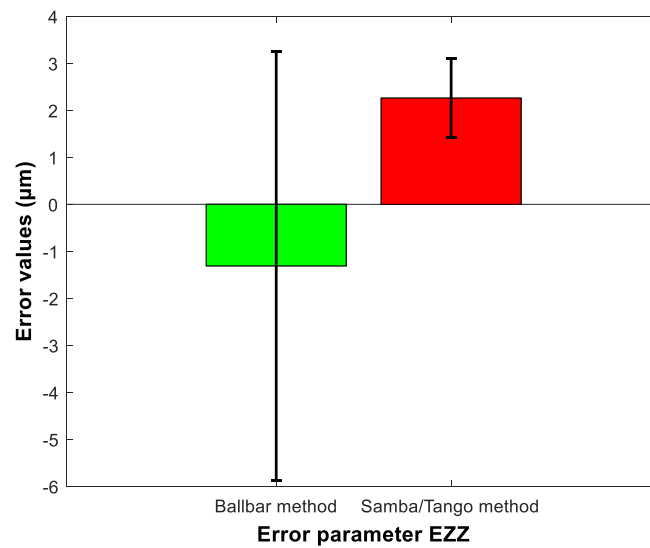
The linear positioning error EZZ by the Renishaw software is in YZ and ZX plane. By Equation 3.5, this is the first-order term in the S/T method while comparing it with the ballbar.

After analyzed Figure 5.17 (a), it is clear that the initial three tests have negative error values and positive error values for both Ball bar and S/T methods, respectively. Suddenly for the last test, it goes positive in the ball bar case.

The mean error value is $-1.31\text{ }\mu\text{m}$ for the ball bar and $2.26\text{ }\mu\text{m}$ by the S/T method. The error range is $3.57\text{ }\mu\text{m}$. The standard deviation is overlap for EZZ, and error values are associated with this parameter. Therefore, the scaling error EZZ is also comparable in both methods.



(a)

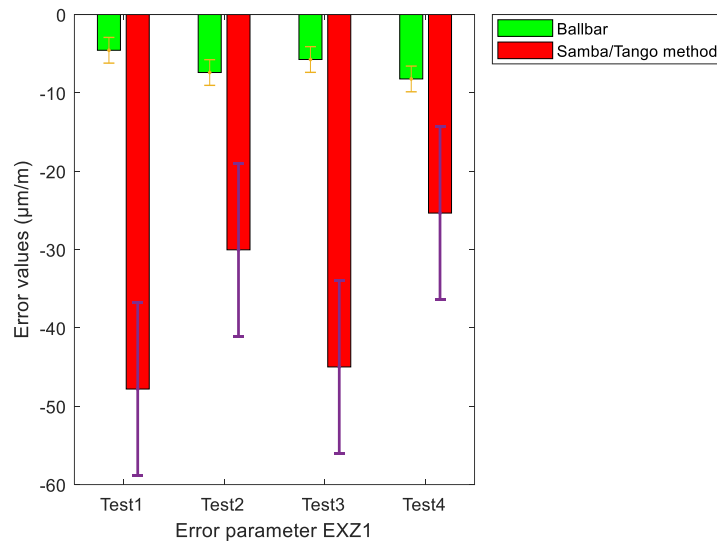


(b)

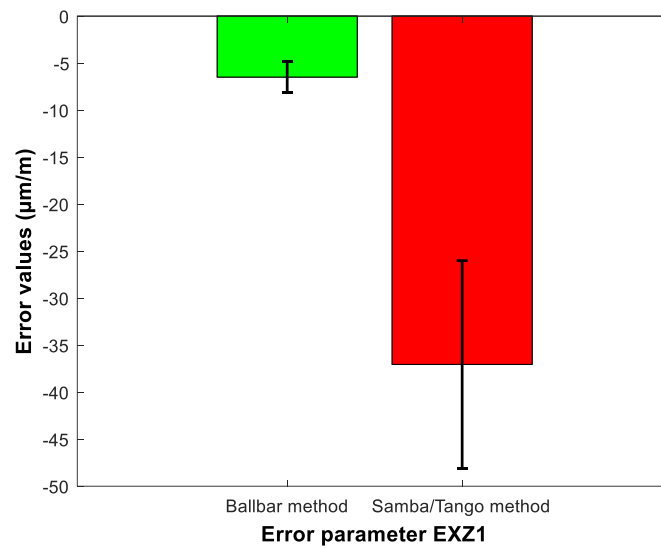
Figure 5.17: Representation of error parameter EZZ

5.1.18 Squareness Error EXZ1

EXZ1 is the second term of the polynomial equation 3.10 and ZX test plane error in the BB experiment. Figure 5.18 (a) presents the analyzed data in a bar graph. The S/T error values are negative for all tests, and ball bar values are also negative, but their value is different.



(a)



(b)

Figure 5.18: Representation of error parameter EXZ1

The mean error value in the BB method is $-6.48 \mu\text{m/m}$, while $-37.04 \mu\text{m/m}$ for the S/T method. Their absolute difference is $30.56 \mu\text{m/m}$, which is the highest difference compare to the other squareness.

The standard deviations are not overlap; the overall observed data is not in adjacent agreement.

5.1.19 Squareness Error ECZ0 and ECX0

Similar to the previous squareness, it is also the first term of the polynomial equation, but in the Renishaw BB test, ECZ0 and ECX0 are XY and YZ test plane error values, respectively.

Figure 5.19 (a) shows that the ECZ0 error value for both methods is positive for all tests, but the S/T measured values are higher compared to the ball bar values.

ECX0 error values shown in Figure 5.19 (b). The ball bar data is positive for all tests, while the S/T method data is negative for three tests, and test 1 value is negligible.

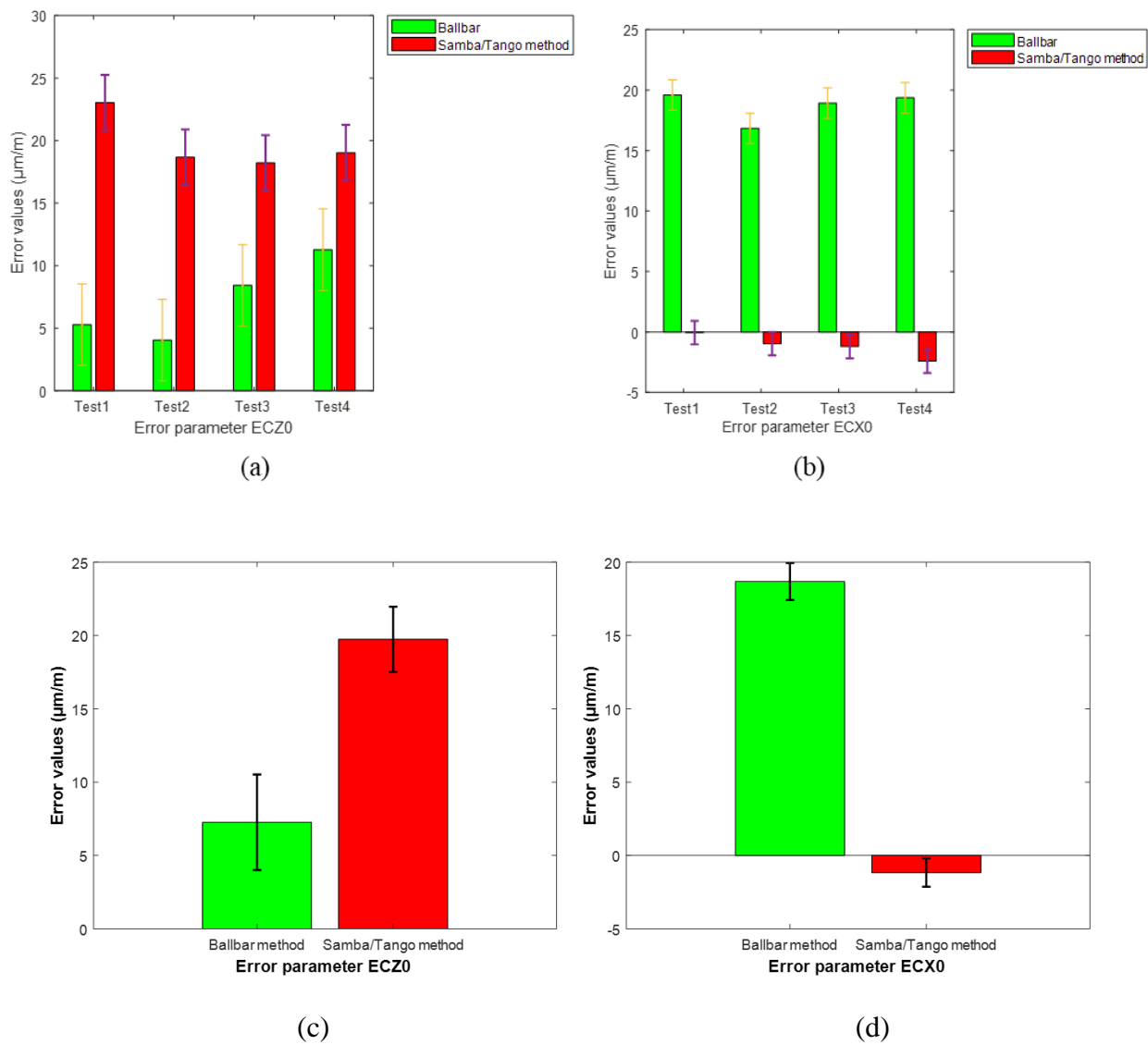


Figure 5.19: Representation of error parameter ECZ0 and ECX0

Figure 5.19 shows both error value for the individual tests as well as their mean values. The ECZ0 error value by the BB is $7.26 \mu\text{m/m}$, and from the S/T method is $19.74 \mu\text{m/m}$, very higher as compared to the BB measured data. Additionally, ECX0 measured value in the S/T method is meager of $-1.17 \mu\text{m/m}$, while for the same parameter, the BB value is $18.68 \mu\text{m/m}$, very high.

For both error parameters, the standard deviation neither overlap nor close to each other as their difference is enormous in the S/T and BB method. These parameter values do not agree with both methods. It seems that ECZ0 and ECX0 are problematic to compare between the two methods.

5.2 Correlation

The main goal of this work is to compare the error parameter in the Renishaw ball bar and S/T method. The data analyzed by applying the correlation between the ball bar method and the S/T method for all twenty-error parameters. The correlation coefficient R used to determine the association between the two methods. As the value of R varies between $-1 \leq R \leq +1$.

When the R -value is $+1$, it means the analyzed data has a strong positive relationship with positive slope. If the R -value is -1 , it shows that analyzed data has a strong negative relationship with a negative slope. As R goes to zero, there is a very tiny connection between the error parameter.

5.2.1 Backlash correlation

Figure 5.19 shows the backlash error correlation between the S/T method and Renishaw analyzed error values. It observed that both parameters have a positive slope where EYYb is highly correlated and near to $+1$.

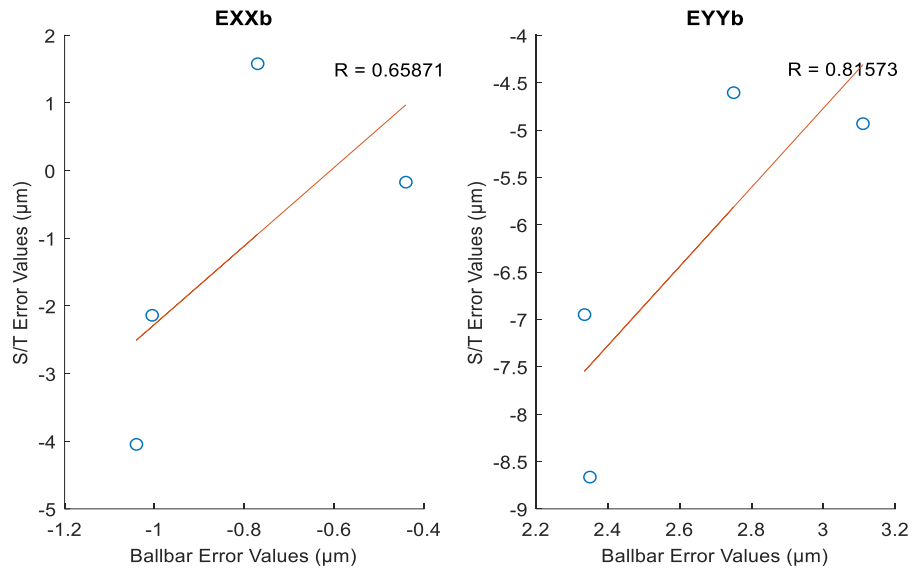


Figure 5.20: Backlash correlation between BB and S/T method

EXXb has a 0.65 correlation coefficient, as observed with four-test measurement. It is less correlated compare to the EYYb because EXXb has a positive error value for the ball bar method while the negative value for the S/T method.

5.2.2 Lateral play correlation

The same method is used to analyses the correlation between S/T and the BB method for lateral play error and correlation presented in Figure 5.20. It has a six-error parameter while comparing both methods.

Figure 5.20 shows the less negative correlation for EXYb reversal error. It is due to the ball bar measured value $0.03 \mu\text{m}$ for test 1 as shown in Table 7.1

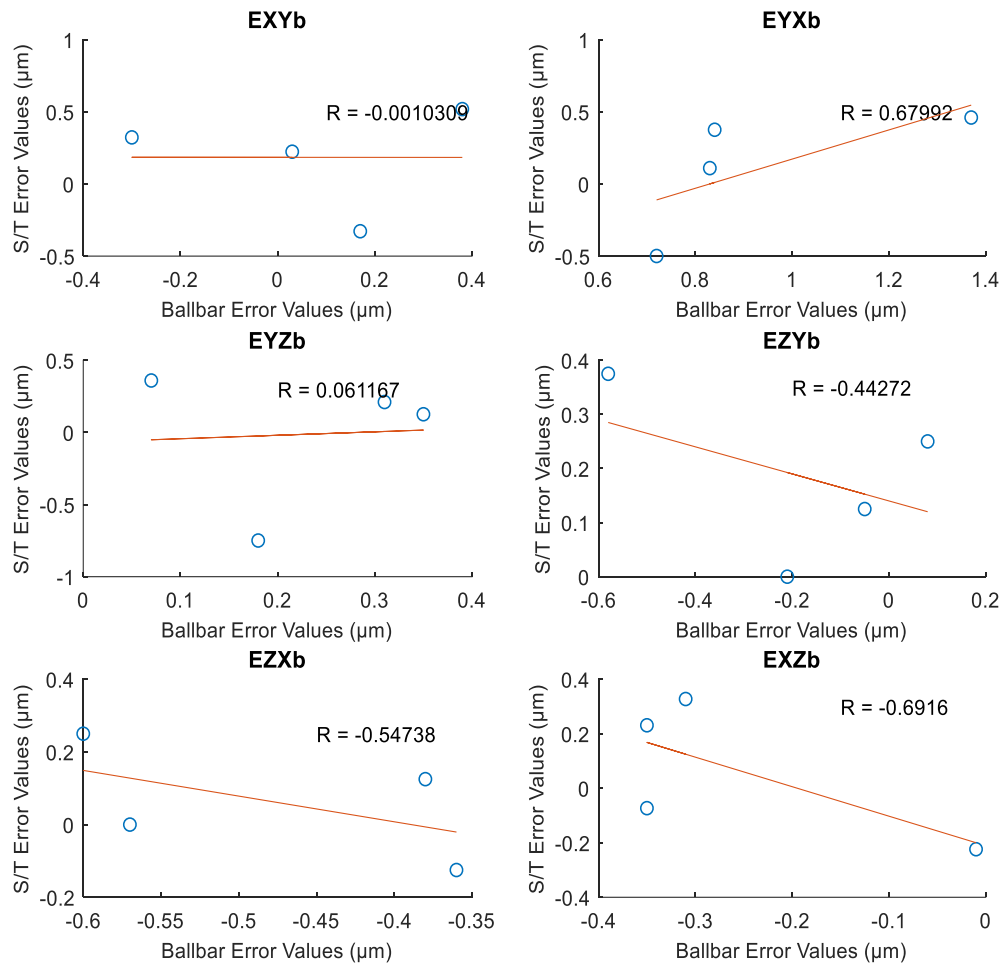


Figure 5.21: Lateral play error correlation between S/T and BB method

EYXb is a reversal error while probing in the y-direction. It has a positive correlation and a comparable parameter in both methods.

The reversal error EYZb is less correlated as it goes to zero R-value. It can summaries that the first test in the S/T method has a negative value compare to the other test in the S/T method. It gives a higher effect when comparing these two methods for this parameter.

The correlation coefficient for EZYb is -0.45. Although their correlation is negative, for the BB and S/T method, their means -0.19 μm and +0.19 μm, respectively, this parameter is associated if neglect the negative sign in the BB approach.

Figure 5.20 illustrates the negative correlation between EZXb and EXZb is -0.5 and -0.7, respectively. Both parameters are less comparable in all-lateral paly errors because of the S/T

method test. In the second test, both have a much-reduced amount of measured value parallel to another test.

5.2.3 Straightness correlation

Figure 5.21 presents the correlation of straightness error between BB and S/T method. Error parameter EYX correlation is positive 0.52, and it is comparable in both techniques.

EZX correlation is 0.14; due to the less positive correlation, this parameter cannot equate in these two methods. From Table 4.2, it is clear that BB means the value is $-0.48 \mu\text{m}$, and the S/T mean value is $-4.22 \mu\text{m}$.

Instead of a high positive correlation 0.72, the error EXY is difficult to show any agreement in the BB and S/T method. Because BB measured error, value is three times higher than the S/T method. On the other hand, EXZ shows a high negative correlation, and it clearly shows in Figure 5.21 that their error parameter means the value is different from each other.

Figure 5.21 shows the EZY and EYZ correlation 0.13 and 0.28, respectively. Although EZY has a positive correlation, their mean value has different sign the BB value is negative, and S/T value is positive if neglect the negative sign in BB measured value, then this parameter is easy to compare.

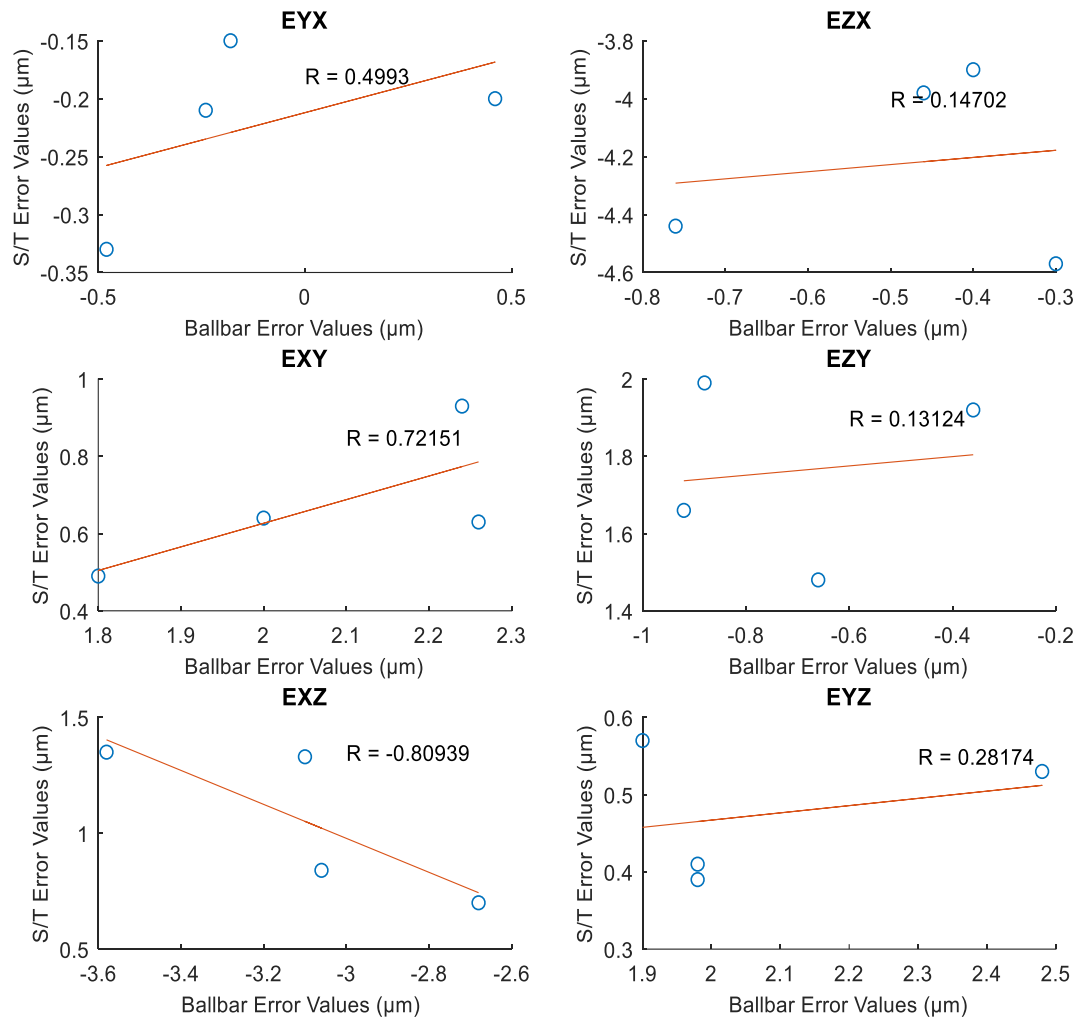


Figure 5.22: Straightness error correlation between S/T and BB method

5.2.4 Scaling error correlation

The correlation from the measured error values shown in Figure 5.22. It is clear from Figure 5.22 that the EXX correlation is negative. It shows less associated data with the BB and S/T method, but from Table 4.2 mean measured value is $-4.65 \mu\text{m}$ and $-4.67 \mu\text{m}$, strictly agreed error parameter in this work. It means higher or less correlation does not prove here that error value can be compared or not.

The y-direction scaling error EYY correlation is -0.66 ; it shows that their experimental data has a negative correlation, but from Table 4.2, their mean value shows a higher difference.

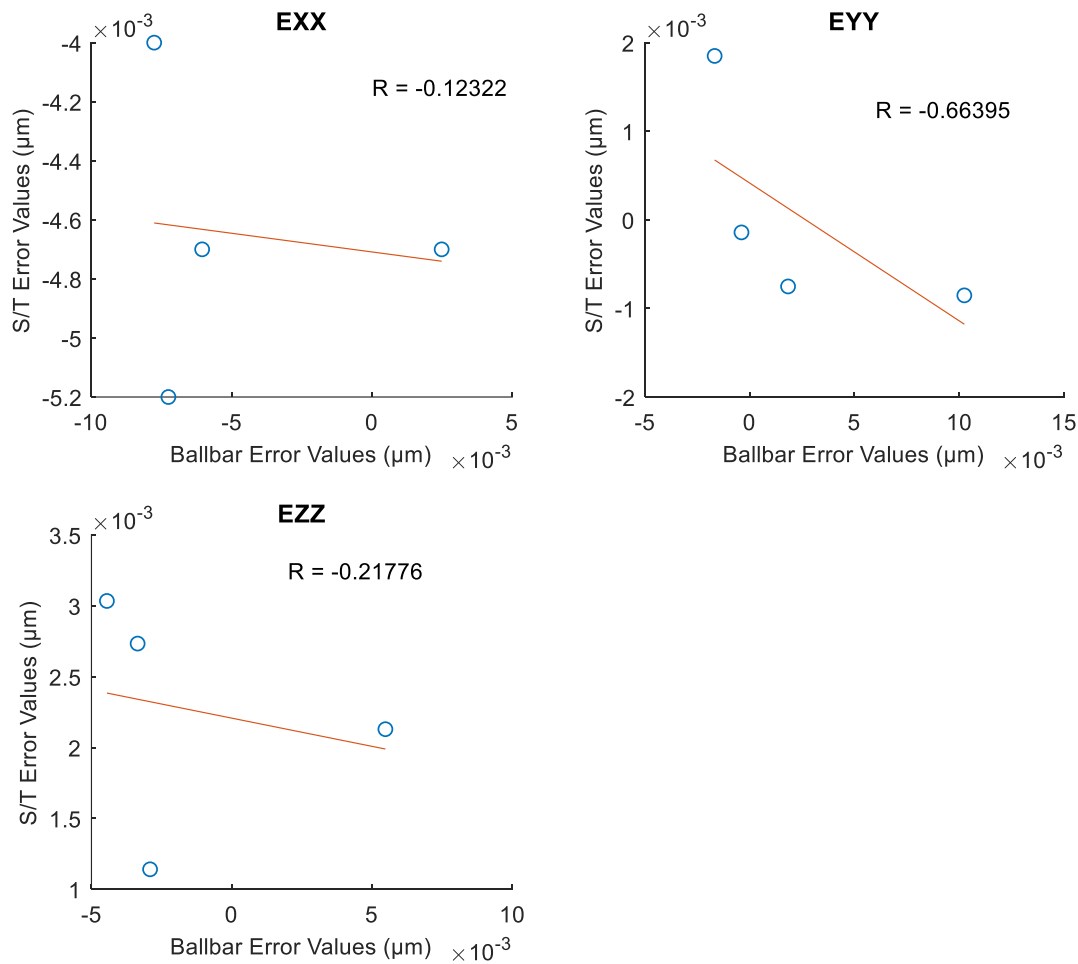


Figure 5.23: Scaling error correlation between S/T and BB method

EZZ correlation coefficient R is -0.21. It shows a negative correlation because BB test measured values have negative signs, while the S/T measured values are in positive sign. If neglect the negative sign in BB measured value, this parameter is equivalent in this work.

5.2.5 Squareness error correlation

ECZ0 and ECX0 have negative correlation, and there mean value is very different from each other. It concludes that these two squareness parameters could not agree in these two methods with the employed strategy.

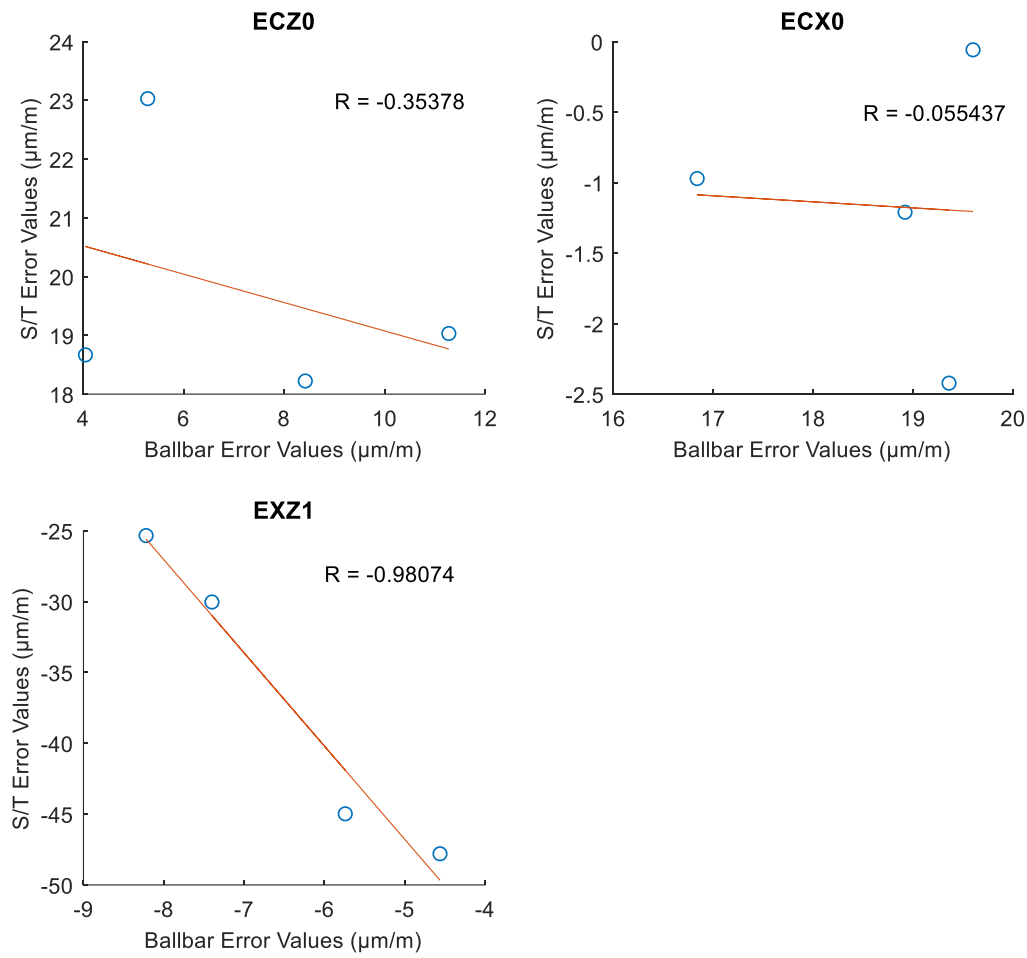


Figure 5.24: Squareness error correlation between S/T and BB method

Figure 5.23 illustrates the correlation coefficient of -0.98 for EXZ1, and the error values do not agree for this parameter.

CHAPTER 6 DISCUSSION

The SAMBA/TANGO and ball bar experimental data were analyzed and graphically presented in the previous chapter. The five-error parameter was selected from the Renishaw ball bar software for different planes such as XY, YZ, and ZX to compare with the SAMBA and TANGO techniques. The selected parameter from the ball bar was backlash error, lateral play error, straightness error, scaling error, and Squareness error.

The strategy designed for the comparison of geometric error has 21 indexations, and one facet was able to intimate the selected parameters. In current work, the combined strategy was developed for SAMBA and TANGO techniques.

It was observed that the scaling error experimental measured values of EXX for the Ball bar and SAMBA/TANGO methods were very close at $-4.65 \mu\text{m}$ and $-4.67 \mu\text{m}$, respectively, with absolute difference $0.03 \mu\text{m}$. Similarly, the error EYY standard deviation was overlapped, but the measured value from the S/T method was negligible around $0.03 \mu\text{m}$ compare to the ball bar measured value. On the other hand, the EZZ standard deviation was overlapped, but their value was in the opposite of both methods.

The reversal error EXYb measured while probing in the x-direction, and it was a significant agreement for the ball bar and SAMBA/TANGO methods as their standard deviation zone overlapped. For similar probing, the error EXZb indicates that the variation of the analyzed result because the obtained value for EXZb was of opposite sign for both methods. The measured error value of reversal error EYZb and EYXb were in acceptable agreement as their standard deviation zone were overlapped. The absolute difference for EYZb and EYXb was $0.25 \mu\text{m}$ and $0.72 \mu\text{m}$ respectively. The estimated standard deviation for EZXb and EZYb was not overlapped, and their values were in opposite sing for two methods; it was challenging to get similar error values for EZXb and EZYb in this study. If neglect the negative sign for the ball bar EZYb parameter, it shows the close agreement for both techniques with $0.57 \mu\text{m}$ difference.

The measured experimental error value for backlash EXXb was in considerable agreement as their standard deviation coincided and their absolute difference was $1.58 \mu\text{m}$, while the EYYb shows an inconsistency of $15.21 \mu\text{m}$, it was a second-highest absolute difference, and the observed error values in the BB and S/T method were in the opposite sign. EYYb was not associated with two

methods. It might be due to the jump in the direction of motion when guideways move in the y-direction.

The straightness error EYX in current work reflects the excellent agreement between the two methods, their absolute difference was $-0.11\text{ }\mu\text{m}$, and the standard deviation zone was overlapped. The straightness EZX, EXY, EXZ, and EYZ exhibit the dissimilarities their standard deviation zone were far from each other as conclusion these straightness were problematic to compare between the BB and S/T methods.

The squareness error EXZ1 was not in considerable agreement because their standard deviation was not in the same zone. The measured value from the BB method was smaller than compared to the S/T method. The error parameter ECZ0 was positive for both methods, but their values were different from each other and for ECX0, the observed error value was in an opposite sign for the BB and S/T technique. Overall, the squareness error was not in clear agreement for XY, YZ, and ZX test plane in selected methods.

Moreover, the backlash error correlation was positive for both methods. EXXb and EYYb correlation were 0.65 and 0.81, respectively, but only EXXb shows a close agreement; the EYYb values were opposite in each method; it was not in agreement.

Instead of -0.001 correlation, the EXYb reversal error was associated with both methods. On the other hand, the EYXb correlation was 0.67, but it did not agree substantially. The error EYZb was in close agreement, but the correlation was 0.061. The correlation of error parameter EZYb, EZXb, and EXZb was around -0.5. These three error parameters measured values were in an opposite sign for the BB and S/T method.

The straightness error EYX was in close agreement with the correlation value of 0.50. The EXZ was in a strong negative correlation -0.80, but it was not in close agreement for this work because it had different error values.

The squareness error EXZ1 correlation was -0.98, and their measured value with both methods was not close to each other. The error ECZ0 and ECX0 correlation were -0.35 and -0.05, respectively. ECZ0 and ECX0 values did not agree.

The correlation analysis shows that if the correlation is strongly positive, it does not prove that the error parameter value is extremely agree for both methods. Similarly, if the correlation is negative or near to zero, it cannot say that error values are not in close agreement.

CHAPTER 7 CONCLUSION AND RECOMMENDATION

The main goal of this research work was to compare the geometric error parameter obtained from the ball bar and SAMBA/TANGO (S/T) methods to determine if they yielded similar results.

The error parameters that could be obtained from both methods were: backlash error, lateral play error, straightness error, scaling error, and squareness errors. A combined strategy was developed for the S/T experiment to get all error parameters. Additionally, the measurement strategy was enriched to estimate the reversal error of the X, Y, and Z-axis. Several experiments were executed for the developed S/T strategy as well as XY, YZ, and ZX plane tests for the Renishaw ball bar to obtain repeatability information.

The result analysis of current work, commands the following conclusion for the comparison of the ball bar and S/T techniques:

- The comparison of the nine-error parameter was possible out of twenty selected error parameters.
- The scaling error EXX was the most agreed parameter in present work, and other scaling error EYY and EZZ agreed as their one standard deviation regions overlapped.
- The developed technique for the reversal error measurement was implemented on the HU40T machine tool and presented reasonable results.
- The reversal error EXYb, EXZb, EYZb, and EYXb were in close agreement as per the standard deviation region, but EZYb and EZXb errors had different sign values in both methods.
- The EXXb backlash was in close agreement with an absolute difference of 1.58 μm . The backlash error EYYb measured values were in opposite sign and not close agreement in the S/T and ball bar methods.
- The straightness error EYX values with absolute difference 0.08 μm were associated with current work. The other straightness EZX, EXY, EZY, EXZ, and EYZ were not in close agreement.
- The squareness error EXZ1, ECZ0, and ECX0 were not showing any agreement for the S/T and ball bar methods.

- The standard deviation considered for the error values agreement, and when the standard deviation overlapped, it was found that the error values were in close agreement for the S/T and ball bar methods. On the other hand, when the standard deviation values were far from each other, meaning that no overlap found, the error values were not in close agreement.
- There was always trouble for the negative sign in the BB method as they were analyzed and obtain by the Renishaw ball bar software, which made some error parameters hard to agree with the BB and SAMBA/TANGO method.

This work was focused on geometric error comparison with the ball bar and SAMBA/TANGO methods, including reversal error measurement. The following future works are suggested as follows:

- It could be exciting to use the laser interferometer technique to compare the error parameter with the indirect method, such as the SAMBA and TANGO method.
- The new technique used in this work for reversal error measurement with X, Y, and Z pre-movement, it will be helpful to provide the pre-movement in A, B, C axis.

REFERENCES

- Abbaszadeh-Mir, Y., Mayer, J. R. R., Cloutier, G., & Fortin, C. (2002). Theory and simulation for the identification of the link geometric errors for a five-axis machine tool using a telescoping magnetic ball-bar. *International Journal of Production Research*, 40(18), 4781-4797. doi:10.1080/00207540210164459
- Bringmann, B., & Knapp, W. (2006). Model-based ‘Chase-the-Ball’ Calibration of a 5-Axes Machining Center. *CIRP Annals*, 55(1), 531-534. doi:https://doi.org/10.1016/S0007-8506(07)60475-2
- Bringmann, B., Küng, A., & Knapp, W. (2005). A Measuring Artefact for true 3D Machine Testing and Calibration. *CIRP Annals*, 54(1), 471-474. doi:https://doi.org/10.1016/S0007-8506(07)60147-4
- Bryan, J. B. (1982). A simple method for testing measuring machines and machine tools. Part 1: Principles and applications. *Precision Engineering*, 4(2), 61-69. doi:https://doi.org/10.1016/0141-6359(82)90018-6
- Chen, J. S., Kou, T. W., & Chiou, S. H. (1999). Geometric error calibration of multi-axis machines using an auto-alignment laser interferometer. *Precision Engineering*, 23(4), 243-252. doi:https://doi.org/10.1016/S0141-6359(99)00016-1
- Erkan, T., Mayer, J. R. R., & Dupont, Y. (2011). Volumetric distortion assessment of a five-axis machine by probing a 3D reconfigurable uncalibrated master ball artefact. *Precision Engineering*, 35(1), 116-125. doi:https://doi.org/10.1016/j.precisioneng.2010.08.003
- Hale, L. C., & Slocum, A. H. (2001). Optimal design techniques for kinematic couplings. *Precision Engineering*, 25(2), 114-127. doi:https://doi.org/10.1016/S0141-6359(00)00066-0
- Hong, C., Ibaraki, S., & Matsubara, A. (2011). *Influence of position-dependent geometric errors of rotary axes on a machining test of cone frustum by five-axis machine tools* (Vol. 35).
- Ibaraki, S., Iritani, T., & Matsushita, T. (2012a). *Calibration of location errors of rotary axes on five-axis machine tools by on-the-machine measurement using a touch-trigger probe* (Vol. 58).
- Ibaraki, S., Iritani, T., & Matsushita, T. (2012b). Calibration of location errors of rotary axes on five-axis machine tools by on-the-machine measurement using a touch-trigger probe.

- International Journal of Machine Tools and Manufacture*, 58, 44-53.
doi:<https://doi.org/10.1016/j.ijmachtools.2012.03.002>
- ISO230-1. (2012). "Test code for machine tools – Part 1: geometric accuracy of machines operating under no-load or quasi-static conditions".
- Jiang, X., & Cripps, R. J. (2015). "A method of testing position independent geometric errors in rotary axes of a five-axis machine tool using a double ball bar". *International Journal of Machine Tools and Manufacture*, 89, 151-158.
doi:<https://doi.org/10.1016/j.ijmachtools.2014.10.010>
- Liebrich, T., Bringmann, B., & Knapp, W. (2009). Calibration of a 3D-ball plate. *Precision Engineering*, 33(1), 1-6. doi:<https://doi.org/10.1016/j.precisioneng.2008.02.003>
- Mayer, J. R. R. (2012). Five-axis machine tool calibration by probing a scale enriched reconfigurable uncalibrated master balls artefact. *CIRP Annals*, 61(1), 515-518. doi:
- Mayer, J. R. R., Rahman, M. M., & Los, A. (2015). An uncalibrated cylindrical indigenous artefact for measuring inter-axis errors of a five-axis machine tool. *CIRP Annals*, 64(1), 487-490.
doi:[10.1016/j.cirp.2015.04.015](https://doi.org/10.1016/j.cirp.2015.04.015)
- Mayr, J., Jedrzejewski, J., Uhlmann, E., Alkan Donmez, M., Knapp, W., Härtig, F., . . . Wegener, K. (2012). Thermal issues in machine tools. *CIRP Annals*, 61(2), 771-791.
doi:<https://doi.org/10.1016/j.cirp.2012.05.008>
- Mchichi, A., & Mayer, R. (2014). *Axis Location Errors and Error Motions Calibration for a Five-axis Machine Tool Using the SAMBA Method* (Vol. 14).
- Rahman, M. M., & Mayer, J. R. R. (2015). Five axis machine tool volumetric error prediction through an indirect estimation of intra- and inter-axis error parameters by probing facets on a scale enriched uncalibrated indigenous artefact. *Precision Engineering*, 40, 94-105.
doi:<https://doi.org/10.1016/j.precisioneng.2014.10.010>
- Renishaw, p. (2001-2019). © 2001-2019 Renishaw plc. All rights reserved. Retrieved from <https://www.renishaw.com/en/ballbar-20-for-qc20-w-and-qc10--11076>
- Schwenke, H., Knapp, W., Haitjema, H., Weckenmann, A., Schmitt, R., & Delbressine, F. (2008). Geometric error measurement and compensation of machines—An update. *CIRP Annals*, 57(2), 660-675. doi:<https://doi.org/10.1016/j.cirp.2008.09.008>

- Srinivasa, N., & Ziegert, J. C. (1996). Automated measurement and compensation of thermally induced error maps in machine tools. *Precision Engineering*, 19(2), 112-132. doi:[https://doi.org/10.1016/S0141-6359\(96\)00042-6](https://doi.org/10.1016/S0141-6359(96)00042-6)
- Weikert, S. (2004). R-Test, a New Device for Accuracy Measurements on Five Axis Machine Tools. *CIRP Annals*, 53(1), 429-432. doi:[https://doi.org/10.1016/S0007-8506\(07\)60732-X](https://doi.org/10.1016/S0007-8506(07)60732-X)
- Xing, K., Achiche, S., Esmaeili, S., & Mayer, J. R. R. (2018). Comparison of Direct and Indirect Methods for Five-axis Machine Tools Geometric Error Measurement. *Procedia CIRP*, 78, 231-236. doi:<https://doi.org/10.1016/j.procir.2018.08.310>
- Xing, K., Achiche, S., & Mayer, J. R. R. (2019, 2019, //). The Effects of Machine Tool Pallet Change on Machine Tool Geometric Measurement Using the Scale and Master Ball Artefact Method (*SAMBA*). Paper presented at the Advances in Engineering Research and Application, Cham.
- Xing, K., Mayer, J. R. R., & Achiche, S. (2018). Machine Tool Volumetric Error Features Extraction and Classification Using Principal Component Analysis and K-Means. *Journal of Manufacturing and Materials Processing*, 2(3), 60. doi:10.3390/jmmp2030060
- Zargarbashi, S. H. H., & Mayer, J. R. R. (2006). Assessment of machine tool trunnion axis motion error, using magnetic double ball bar. *International Journal of Machine Tools and Manufacture*, 46(14), 1823-1834. doi:<https://doi.org/10.1016/j.ijmachtools.2005.11.010>
- Zargarbashi, S. H. H., & Mayer, J. R. R. (2009). Single setup estimation of a five-axis machine tool eight link errors by programmed end point constraint and on the fly measurement with Capball sensor. *International Journal of Machine Tools and Manufacture*, 49(10), 759-766. doi:<https://doi.org/10.1016/j.ijmachtools.2009.05.001>

APPENDICE A EXPERIMENTAL DATA SUMMARY

Table 7.1: Renishaw Ball bar analyzed the result

Error parameter			Test plane	BALL BAR					
				TEST1	TEST2	TEST3	TEST4	Average	Stdev
1	EXXb	BACKLASH (μm)	X	-0.77	-1.005	-1.04	-0.44	-0.81	0.28
2	EYYb		Y	3.11	2.335	2.35	2.75	2.64	0.37
3	EXYb	LATERAL PLAY (μm)	X	0.03	-0.3	0.17	0.38	0.07	0.29
4	EYXb		Y	0.72	0.84	0.83	1.37	0.94	0.29
5	EYZb		Y	0.18	0.35	0.07	0.31	0.23	0.13
6	EZYb		Z	0.08	-0.21	-0.05	-0.58	-0.19	0.29
7	EZXb		Z	-0.6	-0.57	-0.38	-0.36	-0.48	0.13
8	EXZb		X	-0.01	-0.35	-0.31	-0.35	-0.26	0.16
9	EYX	STRAIGHTNESS (μm)	X	-0.24	-0.48	0.46	-0.18	-0.11	0.40
10	EZX		Y	-0.46	-0.3	-0.4	-0.76	-0.48	0.20
11	EXY		Y	2.24	1.8	2	2.26	2.075	0.22
12	EZY		Z	-0.92	-0.88	-0.66	-0.36	-0.71	0.26
13	EXZ		Z	-3.58	-3.06	-3.1	-2.68	-3.11	0.37
14	EYZ	SCALING (μm)	X	1.9	2.48	1.98	1.98	2.09	0.27
15	EXX		XY/ZX	-7.76	-7.26	-6.05	2.48	-4.65	4.81
16	EYY		YZ/XY	-1.67	-0.39	1.83	10.24	2.50	5.36
17	EZZ	SQUARNESS ($\mu\text{m}/\text{m}$)	YZ/ZX	-4.45	-3.35	-2.91	5.48	-1.31	4.57
18	ECZ0		XY	5.28	4.04	8.42	11.28	7.26	3.26
19	ECX0		YZ	19.6	16.84	18.92	19.36	18.68	1.26
20	EXZ1		ZX	-4.56	-7.4	-5.74	-8.22	-6.48	1.64

Table 7.2: SAMBA/ TANGO analyzed the result

Error parameter			Test plane	SAMBA/TANGO					
				TEST 1	TEST 2	TEST 3	TEST 4	Average	Stdev
1	EXXb	BACKLASH (μm)	X	3.16	-4.28	-8.09	-0.34	-2.39	4.87
2	EYYb		Y	-9.87	-13.90	-17.33	-9.21	-12.58	3.79
3	EXYb	LATERAL PLAY (μm)	X	0.45	0.65	-0.66	1.04	0.37	0.73
4	EYXb		Y	-1.00	0.75	0.22	0.92	0.22	0.87
5	EYZb		Y	-1.50	0.25	0.72	0.42	-0.03	1.00
6	EZYb		Z	0.50	0.00	0.25	0.75	0.38	0.32
7	EZXb		Z	0.50	0.00	0.25	-0.25	0.13	0.32
8	EXZb		X	-0.45	-0.15	0.65	0.46	0.13	0.51
9	EYX	STRAIGHTNESS (μm)	X	-0.21	-0.33	-0.20	-0.15	-0.22	0.08
10	EZX		Y	-3.98	-4.57	-3.90	-4.44	-4.22	0.33
11	EXY		Y	0.93	0.49	0.64	0.63	0.67	0.18
12	EZY		Z	1.66	1.99	1.48	1.92	1.76	0.24
13	EXZ		Z	1.35	0.84	1.33	0.70	1.05	0.33
14	EYZ		X	0.57	0.53	0.39	0.41	0.48	0.09
15	EXX	SCALING (μm)	XY / ZX	-4.00	-5.23	-4.74	-4.74	-4.67	0.50
16	EYY		YZ / XY	1.85	-0.14	-0.75	-0.85	0.03	1.26
17	EZZ		YZ / ZX	3.03	2.73	1.14	2.13	2.26	0.84
18	ECZ0	SQUARNESS ($\mu\text{m}/\text{m}$)	XY	23.03	18.67	18.22	19.03	19.74	2.22
19	ECX0		YZ	-0.06	-0.97	-1.21	-2.42	-1.17	0.97
20	EXZ1		ZX	-47.80	-30.03	-44.98	-25.34	-37.04	11.03